# SUBSURFACE RESISTIVITY INVESTIGATION AT THE CENTRE FOR ENERGY RESEARCH AND TRAINING (CERT), AHMADU BELLO UNIVERSITY, ZARIA, NIGERIA.

**BY**


## FADELE SUNDAY IDOWU

**DEPARTMENT OF PHYSICS**
**AHMADU BELLO UNIVERSITY, ZARIA.**


**JUNE, 2011.**

# SUBSURFACE RESISTIVITY INVESTIGATION AT THE CENTRE FOR ENERGY RESEARCH AND TRAINING (CERT), AHMADU BELLO UNIVERSITY, ZARIA, NIGERIA.

**BY**

**FADELE SUNDAY IDOWU** **B.Sc (NSUK 2006)**
**M.Sc/SCIEN/10628/07-08**

**A THESIS SUBMITTED TO THE POSTGRADUATE SCHOOL, AHMADU BELLO UNIVERSITY, ZARIA, NIGERIA**

**IN PARTIAL FULFILMENT FOR THE AWARD OF MASTERS OF SCIENCE IN APPLIED GEOPHYSICS**

**DEPARTMENT OF PHYSICS**
**AHMADU BELLO UNIVERSITY, ZARIA.**

**JUNE, 2011.**

## DECLARATION

I declare that the work in the thesis titled '***SUBSURFACE RESISTIVITY INVESTIGATIONS AT THE CENTRE FOR ENERGY RESEARCH AND TRAINING, AHMADU BELLO UNIVERSITY, ZARIA, NIGERIA'***, has been performed by me in the Department of Physics under the supervision of Dr. P.O. Sule and Dr. B.B.M. Dewu. The information derived from the literature has been duly acknowledged in the text and a list of references provided. No part of this thesis was previously presented for another degree or diploma at any university.

| Fadele Sunday Idowu | | |
|---|---|---|
| --- | --- | --- |
| Name of student | Signature | Date |

## CERTIFICATION

This thesis titled '***SUBSURFACE RESISTIVITY INVESTIGATIONS AT THE CENTRE FOR ENERGY RESEARCH AND TRAINING, AHMADU BELLO UNIVERSITY, ZARIA, NIGERIA'*** meets the regulations governing the award of Masters degree of Science of Ahmadu Bello University, Zaria and is approved for its contribution to knowledge and literary presentation.

| | | |
|---|---|---|
| ---------- | …… | ---------- |
| Chairman, Supervisory Committee<br>Dr. P.O. Sule | Signature | Date |
| ---------- | …… | ……. |
| Member, Supervisory Committee<br>Dr. B.B.M. Dewu | Signature | Date |
| ---------- | ---------- | …… |
| Head of Department<br>Dr. R. Nasiru | Signature | Date |
| ---------- | ---------- | ……... |
| Dean, Postgraduate School<br>Prof. J.A. Abiodun | Signature | Date |

## DEDICATION

I dedicate this work to these two families: Fadele and Bamigboye's family and to my little niece and nephew, Oluwafisayo and Ayomide. I'm pleased to have you guys.

## ACKNOWLEDGEMENT

I thank the almighty God for successfully sailing me through the rigour of this resourceful research work.

I express my profound gratitude to Dr. P.O. Sule who supervised the research work. I appreciate not only his assiduity, painstaking and enduring attitudes to my disturbing 'learner type' questioning habits in order to ensure the successful completion of this work, but also for his fatherly contributions in various forms to make this work a huge success. May God reward him accordingly.

I equally thank Dr. B.B.M. Dewu for his easy going and approachable attitudes to me with numerous suggestions and academic contributions in the course of this study.

Special thanks to my dearest mum Mrs. R. Fadele and my big sister Mrs. I.D. Bamigboye, for their financial and morale support from the beginning of this programme to date. Indeed you are great but I wish you a greater height in life.

The efforts of the following eminent individuals are equally cherished: Dr. C. Collins, Dr. U. Sadiq, Dr. K. Lawal, Mr. Nwosu of the Department of Physics, Dr. P. Ogunleye, Madam Obasi of Centre for Energy Research and Training, Ahmadu Bello University, Zaria. I appreciate you all.

I express my gratitude to the fans of my achievements: foremost among who is my mum and eldest sister, then the rest of my family members and of course my friends. A special thanks to Olaniyi Oluwayemisi for her supports throughout the work and to my colleagues: Jatto, George, C.Y, Mamman 'auntie', John, Danbam, Ritji, Ekeate and Alfa. You are wonderful people, God bless you all.

That a name is not mentioned here is not meant to disregard your contributions in whatever form, but the omission is as a result of space constraint. Please pardon me and thank you all.

## ABSTRACT

Electrical resistivity method was used in carrying out geophysical investigations at the Centre for Energy Research and Training (CERT), Ahmadu Bello University, Zaria, with a view to determining the depth to the bedrock, thickness of weathered basement and the structural deformation of the subsurface rocks. The Vertical Electrical Sounding (VES) using Schlumberger array was carried out at forty (40) stations. ABEM terrameter (SAS 300) was used for the data acquisition. The field data obtained were analysed using a computer software (IPI2win) which gives an automatic interpretation of the apparent resistivity data. Results from the interpretation suggest three (3) layers in most parts of the study area. However, there is a case of two (2) layers at a station. The resistivity value for the topsoil varies from 2 to 738Ωm with thickness ranging from 1.00 to 3.90 metres. The weathered basement has resistivity values ranging from 32 to757Ωm and thickness of between 0.52 and 23.00 metres. The fresh basement (bedrock) has resistivity values as high as 6,036Ωm. The topsoil is characterized by fine grain rocks (clayey), associated with weathering of sulphide minerals from the underlying granitic rocks. They have great amount of dissolved salts resulting to their low resistivity values. The weathered basements are medium to fine grain, porous or fractured rocks containing water. They are referred to as the aquiferrous zone. Highly fractured areas here have low resistivity because of its high degree of saturated water implying that their resistivity is greatly influenced by underground water. The geologic sections derived, suggest that the weathered basement entirely represent a promising aquifer which can serve as the source of water to the area throughout the year. The fresh basement rocks are coarse, close grained (plutonic or intrusive) rocks, constituting the rock forming minerals which are poor conductors resulting to their high resistivity values. The parameters of investigation have helped in identifying

strategic areas for siting high-rise buildings, potential positions for the siting of boreholes and possible depth of sewage system in order to avoid groundwater contamination since the area is generally a shallow fresh basement. A borehole log was provided for the only borehole present in the area. Azimuthal sounding plots have revealed the existence of resistivity anisotropies, trending NW-SE, NE-SW and E-W directions. These structural trends conform with the Orogenic events that took place in the Basement Complex of Nigeria, implying that the study area was affected by the two major Orogenic events that took place in the Nigeria Basement Complex, that is, the Pan-African (600 ma) and Eburnean Orogeny (1950±50 ma).

## TABLE OF CONTENTS

**Page**

**COVER PAGE**

**TITLE PAGE**……ii

**DECLARATION**……...iii

**CERTIFICATION**……iv

**DEDICATION**……v

**ACKNOWLEDGEMENT**……vi

**ABSTRACT**……vii

**TABLE OF CONTENTS**……...ix

**LIST OF TABLES**.....xii

**LIST OF FIGURES**……xiii

**LIST OF APPENDICES**……xiv

**ABBREVIATION, SYMBOLS AND DEFINITIONS**……xvi

**CHAPTER ONE**……1

**INTRODUCTION**……..1

1.1 Preamble……1

1.2 Climate, Vegetation and Geomorphology of the Study Area……...2

1.3 Aim and Scope of the Study…….…....6

1.4 Limitations…….....6

1.5 Justification……7

**CHAPTER TWO**……....8

**LITERATURE REVIEW**…….....8

2.1 Previous Geophysical investigations……....8

2.2 Related Previous Studies ……..…...8

2.3 Geology of the Study Area…….....9

2.3.1 Migmatite-Gneiss Complex……...12

2.3.2 Schists Belts……...13

2.3.3 The Older Granites…….....13

2.4 Structural Geology of the Study Area…….....15

**CHAPTER THREE**…….....16

**METHODOLOGY**……....16

3.1 Field-Work Planning……...…...16

3.1.1 Choice of Electrode Configuration……...…..…16

3.1.2 Resistivity Values of Rocks and Minerals……...……18

3.1.3 Electrical Properties of Earth materials and Parameters……...21

3.1.3.1 Electrical Conductivities……...21

3.1.3.2 Electrical Potentials……...24

3.1.3.3 Dielectric Constant of rocks and minerals…….....26

3.1.3.4 Magnetic Permeabilty……26

3.1.4 Data Collection……27

3.1.5 Instrumentation……...…….....27

3.2 Basis and Theory of the Method used……..28

3.2.1 Basis of D.C. Resistivity Method…….....28

3.2.2 Theory of D.C. Resistivity Method…….....28

3.3 Data Reduction……..……..31

3.4 IPI2win Model overview…….....32

3.4.1 Data Managing……32

**CHAPTER FOUR**……35

**INTERPRETATION OF RESULTS AND DEDUCTIONS**…….....35

4.1 General Statement…….....35

4.1.1 Interpretation……..36

4.2 Results and Deductions from the VES Data…….....44

4.2.1 Geoelectric Sections along Profiles……....44

4.2.2 PROFILE AB……45

4.2.3 PROFILE CD……46

4.2.4 PROFILE EF…….....46

4.2.5 PROFILE GH…….....46

4.2.6 PROFILE IJ……....…47

4.2.7 PROFILE KL…….....47

4.2.8 PROFILE MN…….……48

4.2.9 Isoresistivity Contour Maps…….52

4.2.10 Results From Azimuthal Sounding Plots…….....57

4.2.11 Depth to Bedrock Map……...60

4.2.12 Depth to and Thickness of Weathered Basement Maps…….64

**CHAPTER FIVE**……..67

**DISCUSSION OF RESULTS, CONCLUSION AND RECOMMENDATION**……67

5.1 General Discussion of results……67

5.3 Conclusion…….....69

5.4 Recommendation……...70

**REFERENCES**……...71

**APPENDIX**……75

## LIST OF TABLES

Table 1.1 Some Geophysical Methods, their measured Parameters and Operative Physical Properties……..1

Table 4.1 The Results of the Interpreted VES Curves……39

Table 4.2 Resistivities of some Igneous, Metamorphic and Sedimentary rocks……43

Table 4.3 Resistivity Values adopted for this Work……43

Table 4.4 Lithology and Aquifer Borehole 2 – Amina Hostel, Ahmadu Bello University….45

Table 4.5 Trends of Subsurface Resistivity Anisotropies as obtained from the Azimuthal Sounding Plots…….59

## LIST OF FIGURES

Fig. 1.1 Part of Zaria Sheet 102 Map Showing the Study area…….4

Fig. 1.2 The Study area showing Physical Development……..5

Fig. 2.1 Outline Geological Map of Nigeria……11

Fig. 3.1 VES stations in the Study area……...17

Fig. 3.2 Schlumbeger Array…….29

Fig.4.1 VES Curve at Station CT1……...37

Fig.4.2 VES Curve at Station CT3……...37

Fig.4.3 VES Curve at Station CT5……...37

Fig.4.4 VES Curve at Station CT10…….38

Fig.4.5 VES Curve at Station CT34..……...38

Fig. 4.6 Geologic Sections Derived from Geoelectric data along profiles AB, CD and EF…49

Fig. 4.7 Geologic Sections Derived from Geoelectric data along profiles GH, MN, IJ and KL……50

Fig. 4.8 Isoresistivity Map at 2.00m depth……...52

Fig. 4.9 Isoresistivity Map at 5.00m depth……...53

Fig. 4.10 Isoresistivity Map at 10.00m depth……...54

Fig. 4.11 Isoresistivity Map at 20.00m depth……...55

Fig. 4.12 Isoresistivity Map at 25.00m depth……...56

Fig.4.13 Plots of Azimuthal Sounding at Stations CT12, CT15, CT18 and CT22……..58

Fig.4.14 Depth-to-Bedrock Map……..61

Fig. 4.15 Surface Plot of the Bedrock……..63

Fig. 4.16 Depth-to-Weathered Basement Map…….65

Fig. 4.17 Thickness-of-Weathered Basement Map……..66

## LIST OF APPENDICES

CURVE RESULT AT VES CT1……..75

CURVE RESULT AT VES CT2……..75

CURVE RESULT AT VES CT3……..75

CURVE RESULT AT VES CT4……..76

CURVE RESULT AT VES CT5……..76

CURVE RESULT AT VES CT6……..76

CURVE RESULT AT VES CT7……..77

CURVE RESULT AT VES CT8……..77

CURVE RESULT AT VES CT9……..77

CURVE RESULT AT VES CT10……....78

CURVE RESULT AT VES CT11……78

CURVE RESULT AT VES CT12……78

CURVE RESULT AT VES CT13……79

CURVE RESULT AT VES CT14……79

CURVE RESULT AT VES CT15……79

CURVE RESULT AT VES CT16……80

CURVE RESULT AT VES CT17……80

CURVE RESULT AT VES CT18……80

CURVE RESULT AT VES CT19……81

CURVE RESULT AT VES CT20……81

CURVE RESULT AT VES CT21……81

CURVE RESULT AT VES CT22……82
CURVE RESULT AT VES CT23……82
CURVE RESULT AT VES CT24……82
CURVE RESULT AT VES CT25……83
CURVE RESULT AT VES CT26……83
CURVE RESULT AT VES CT27……83
CURVE RESULT AT VES CT28……84
CURVE RESULT AT VES CT29……84
CURVE RESULT AT VES CT30……84
CURVE RESULT AT VES CT31……85
CURVE RESULT AT VES CT32……85
CURVE RESULT AT VES CT33……85
CURVE RESULT AT VES CT34……86
CURVE RESULT AT VES CT35……86
CURVE RESULT AT VES CT36……86
CURVE RESULT AT VES CT37……87
CURVE RESULT AT VES CT38……87
CURVE RESULT AT VES CT39……87
CURVE RESULT AT VES CT40……88

## ABBREVIATIONS, SYMBOLS AND DEFINITIONS

| | |
|---|---|
| CERT | Centre for Energy Research and Training |
| VES | Vertical Electrical Sounding |
| CT | Station |
| FIG | Figure |
| M | Metre |
| KM | Kilometer |
| N-E | North-East |
| E-W | East-West |
| NW-SE | Northwest-Southeast |
| NE-SW | Northeast-Southwest |
| Ω | Ohms |
| Ωm | Ohm-metre |
| ° | Degree |
| ′ | Minute |
| ″ | Second |
| ρ | True resistivity |
| $\rho_a$ | Apparent resistivity |
| mV | Millivolt |
| I | Current |
| A | Cross sectional area |
| V | Electrical current |
| L | Length |
| K | Geometric factor |
| MN | Potential electrode separation |

| | |
|---|---|
| AB | Current electrode separation |
| $\pi$ | Pi (= 3.1416) |
| i.e | That is |
| et al | And others |
| % | Percentage |
| $\sigma$ | Conductivity |
| $j$ | Current density |
| $E$ | Electric field |
| $\phi$ | Fractional pore volume (porosity) and Adsorption (zeta) potential |
| S | Fraction of the pores containing water |
| $\rho_w$ | Resistivity of water |
| kHz | Kilohertz |
| K | Dielectric constant and Magnetic susceptibility |
| $\eta$ | Viscocity |
| $\Delta P$ | Pressure difference |
| $\varepsilon$ | Solution dielectric constant |
| $R$ | Gas constant (8.31 joules/℃) |
| $F$ | Faraday constant (9.65 x $10^4$ C/mol) |
| $I_a$ and $I_c$ | Mobilities of anions and cations |
| $C_1$ and $C_2$ | Solution concentrations |
| $\theta$ | Absolute temperature |
| n | Valence |
| $\mu$ | Magnetic permeability |

# CHAPTER ONE

# INTRODUCTION

## 1.1 Preamble

Geophysics is a branch of science that applies physical principles to the study of the earth. Many geophysical surveying methods exist, and each method has an operative physical property to which the method is sensitive. Some of the geophysical methods are shown in Table 1.1.

Table 1.1: **SOME GEOPHYSICAL METHODS, THEIR MEASURED PARAMETERS AND OPERATIVE PHYSICAL PROPERTIES**.

| **Method** | **Measured parameter** | **Operative physical property** |
|---|---|---|
| Seismic | Travel times of reflected/refracted seismic waves. | Density & elastic moduli, which determine the propagation velocity of seismic waves. |
| Gravity | Spatial variation in the strength of the gravitational field of the earth. | Density |
| Magnetic | Spatial variation in the strength of the geomagnetic field. | Magnetic susceptibility & remanence. |
| Resistivity | Earth resistance. | Electrical conductivity. |
| Induced polarization | Polarization voltages or frequency-dependent ground resistance. | Electrical capacitance. |
| Self potential | Electrical potential. | Electrical conductivity |
| Electromagnetic | Response to electromagnetic radiation. | Electrical conductivity & inductance. |

The electrical methods are generally classified according to the energy source involved, i.e., natural or artificial. Thus, self potential (SP), telluric current, magnetotelluric (MT) and audio frequency magnetic field (AFMAG) methods come under natural source methods, while resistivity, equipotential, mise-å-la-masse, electromagnetic (EM) and induced polarization (IP) methods are artificial source methods.

In this work, the electrical d.c. resistivity method was used in carrying out geophysical investigation of the Centre for Energy Research and Training (CERT), Ahmadu Bello University, Zaria. The parameters investigated in this area include the depth to the bedrock, distribution of the weathered basement rocks and the subsurface deformational rock systems.

**1.2 Climate, Vegetation and Geomorphology of the Study Area**

Centre for Energy Research and Training, Ahmadu Bello University, Zaria is located in the South-Western region of the Zaria Sheet 102 map (Fig. 1.1). The study area is bounded approximately by longitudes $7^0$ 38′58″ E and $7^0$42’15”E and latitudes $11^0$08’35’’N and $11^0$08’58’’N within the Zaria Sheet 102 SW map. Zaria lies in the Guinea Savannah, woodland vegetation characterized by bushes generally less than 3 metres high and scattered trees. The vegetation assumes various shades of green in the wet season and turns brown or pale in the dry season. Extensive farming usually takes place during the rainy season, but with the presence of rivers like the Kubanni, irrigation farming system is also practised in some areas.

The study area can be reached through the federal high way of Sokoto – Zaria road.

The study area falls within the semi-arid zone of Nigeria (Harold, 1970). The mean annual rainfall over a period of 35 – 40 years for Zaria is 109.2 mm (Olufemi, 1985). From middle to the end of April marks the beginning of perennial rainfall and it ends late October or

very early November. The greatest rainfall usually comes in August. The harmattan period, marking the coldest period, with temperatures between $20^0$C and $30^0$C, starts in late December (Olufemi, 1985). The hottest period is in March with temperature rising above $35^0$C. Groundwater occurrence in the study area is therefore, not only a consequence of hydrologic and geologic events, but also of the climatic (rainfall) conditions. Invasion of two (2) air masses are witnessed here; the northern air mass that is dry and continental in origin, and the southern air mass which is moist, this is known to come from the Atlantic. This latter air mass, which is cold, is maritime in nature (Thorp, 1970).

The drainage system of Zaria is influenced by the Galma River, a major tributary to River Kaduna. It flows towards north, while the Kubanni river flows eastward. The Galma and Kubanni rivers have water thoughout the year unlike their smaller tributaries that are seasonal (Thorp, 1970).

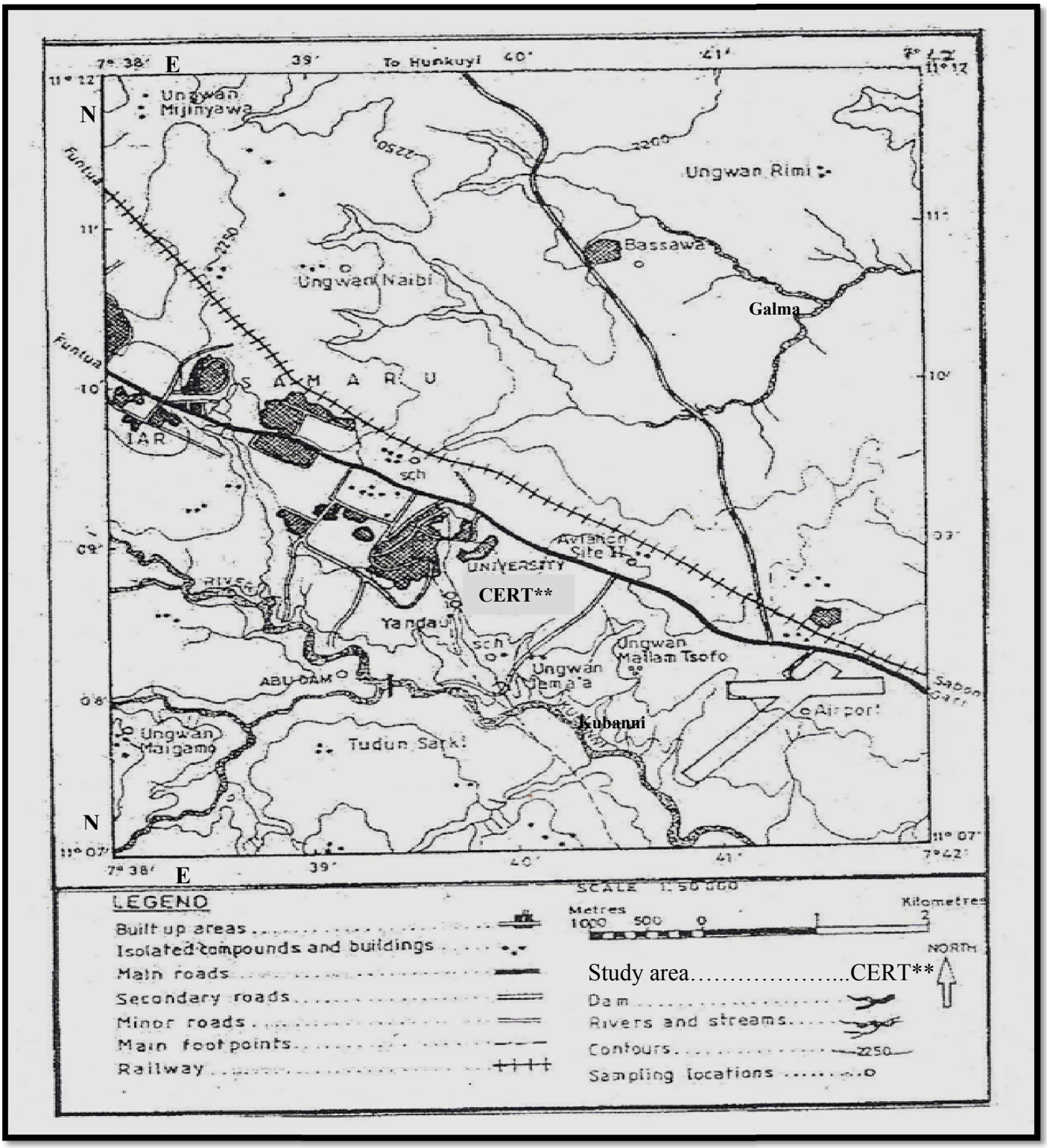



**FIG 1.1: PART OF ZARIA SHEET 102 MAP SHOWING THE STUDY AREA. (Drawn from Northern Nigerian Survey Map).**

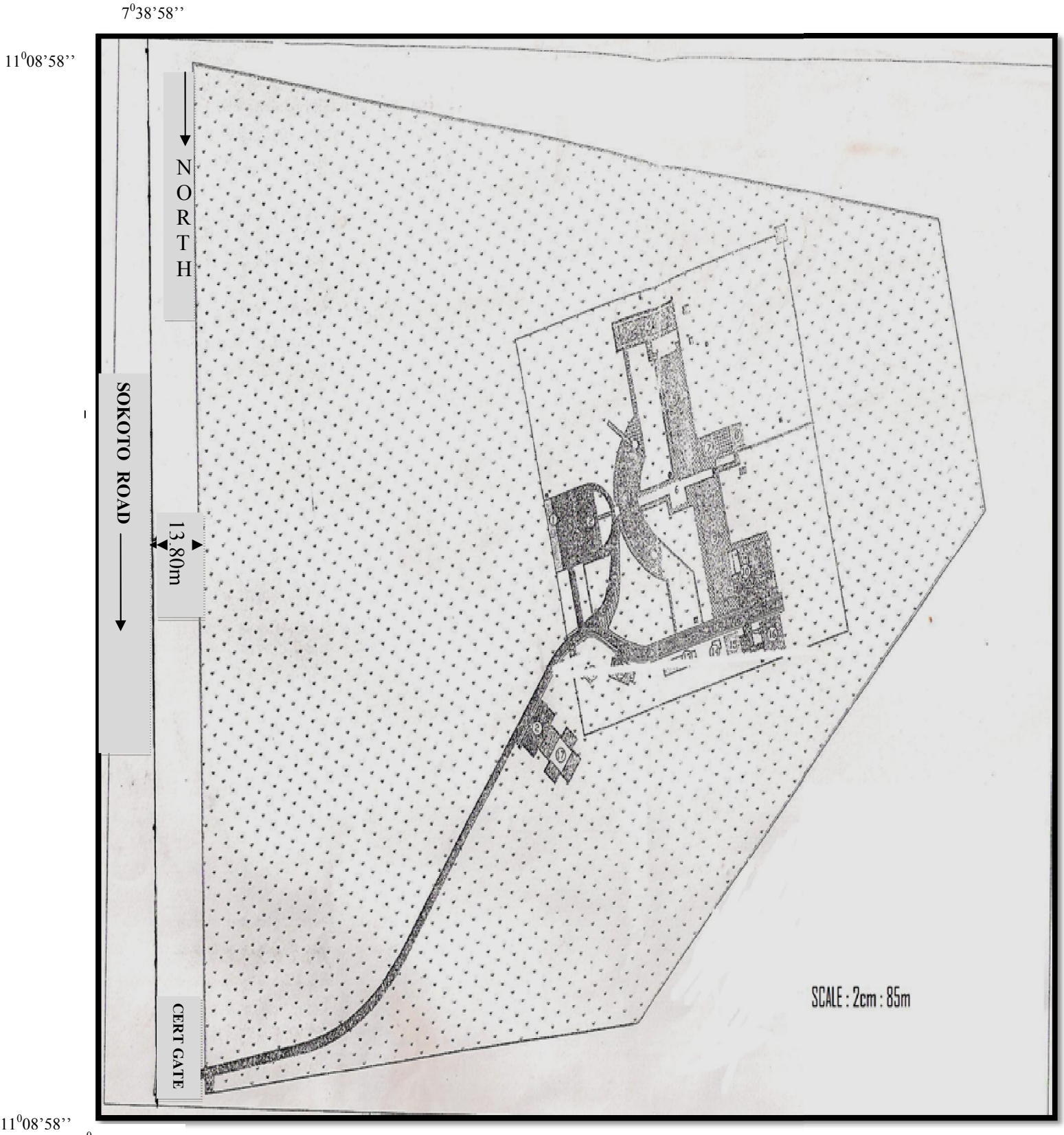



**FIG. 1.2: THE STUDY AREA SHOWING PHYSICAL DEVELOPMENT.**
**(from CERT Site Plan, 2009)**

### 1.3 Aim and Scope of the Study

Electrical Resistivity investigations have been carried out at the Centre for Energy Research and Training, Ahmadu Bello University, Zaria. The work is aimed at;

i. Determining the depth to bedrock,

ii. Thickness of the weathered basement distribution and

iii. Structural deformational trend of the subsurface rocks in the study area.

The Vertical Electrical Sounding (VES) using Schlumberger array was used at forty (40) VES stations and all the necessary information about the parameters of interest used as interpretation aid was provided by computer software (IPI2win). The work also aimed at:

iv. Identifying strategic areas for siting high-rise buildings,

v. Potential positions for the location of boreholes and

vi. Possible depth of sewage system in order to avoid groundwater contamination.

### 1.4 Limitations

It was not possible to lay out regular grid at the Main building of the study area as a result of some physical developments such as, fences and buildings; however, strategic stations were selected for the sounding points.

Another limitation here was the practical difficulty involved in dragging the wires over tall grasses, which slowed down the pace of work.

## 1.5 Justification

The study area Centre for Energy Reasearch and Training, Ahmadu Bello University, Zaria is situated on the Basement Complex rock of north western Nigeria with variable overburden thicknesses. Owing to the fixed nature and size of the site (about $1Km^2$), it is expected that in the nearest future, developments which may include erection of high-rise buildings either for staff or expansion of the current building as a result of the strategic role this research institute plays both in academic and research work of the University and nation at large. There is therefore, the need to provide information on the subsurface sequence and structural disposition necessary for the building. Detailed geophysical investigation provides such information.

Again, as staff population and structures increases, pressure will be mounted on the only existing borehole. As such, it becomes imperative to locate other potential positions suitable for siting boreholes to supplement the existing one. This no doubt will help avert shortage of water at the Centre.

It is also important to know the depth to aquifer especially when constructing sewage system in order to avoid groundwater contamination. Since no reported subsurface investigation has been done here, this work shall provide the following results; depth to bedrock, thickness of weathered basement (aquiferous zone) and the deformational trend of the subsurface rocks at the site.

# CHAPTER TWO

# LITERATURE REVIEW

## 2.1 Previous Geophysical Investigations

Apart from the work done by the Ministry of Water Resources, Kaduna, in siting a borehole at a point in the study area, this work is the basis of a reported geophysical work for further studies covering an area extent of about $1Km^2$. A remarkable work in the area is the aeromagnetic survey project carried out throughout the country by the geological survey of Nigeria in 2009. This has led to the production of nation-wide aeromagnetic maps used for geophysical studies.

Work done by Danladi (1985), appraising the hydrogeology in Zaria has confirmed the presence of water-bearing fractures, which aquifers are located at shallow basement areas of Zaria. Similarly, Hassan (1987) has reported from the VES data he acquired from the Kubanni Basin that the bedrock is undulating, with depths of burial increasing towards the Kubanni river.

## 2.2 Related Previous Studies

Olowu (1967), carried out a regional study of the Zaria Sheet 102 SW map and revealed that with the exception of Galma River, all streams in the area were seasonal and that the depth to water-table increased progressively away from the banks of the river during dry season. He also reported the occurrence of groundwater in joints, weathered portion of basement complex and in overlying alluvium. Eigbefo (1978) not only confirmed that the depths to water-table at various points in the Kubanni basin ranged between 3.00 and 10.00m, he also found the range of thickness of the weathered basement to be 1.00 to 30.00m.

Farouq (2001), showed from his geoelectric investigation of the groundwater potential in the Institute for Agricultural Research farm, Samaru, Zaria that the thickness of the weathered basement around the area varied from about 3.40m to about 30.40m and the depth to fresh basement was about 40.00m.

Saminu (1999), who carried out a comprehensive geophysical survey in the premises of Federal College of Education, Zaria, has shown that the resistivity value for the topsoil varies from 30 to 300 ohm-metres with a thickness ranging between 3.50 and 14.00m. The weathered basement has resistivity values of 84 to 480 ohm-metres and thickness of between 9.00 and 36.50m. The depth to the bedrock varies from 5.00 to 14.00m with resistivity value as high as 3,000 ohm-metres.

McCurry (1970), who studied the geology of Zaria, has established that the Basement Complex rock is made up of Older Granite and Biotite Granite Gneiss. Klinkenbera (1970) has classified the soils in Zaria under leached ferruginous tropical soils. According to him, the soil is weakly developed near inselbergs and hydromorphic soils and formed fadama soils and that the soils contain about 40% clay at some depths.

Hore (1970), has established that Zaria has tropical continental climate that is most prominent in the dry seasons- around December and January. He has shown the mean daily temperature to be $31^0$C with minimum and maximum temperature values ranging between $26^0$C and $36^0$C. He concluded by giving 108.8mm as the mean annual rainfall in Zaria.

**2.3 Geology of the Study Area**

The study area is a Basement Complex terrain and is part of the "Zaria Batholiths". A thick overburden covers the area with varying thicknesses. Underlying the overburden are crystalline rocks consisting of biotite-hornblende granite. The granites belong to the Older

Granites suite of the North-Western Nigeria, emplaced during the Pan-African events that took place about 600 million years ago (McCurry, 1970).

The Nigeria Basement Complex rocks outcrop in nearly half of the country, covering almost all of the south western part of the country. It also covers a wide proportion of the north central part (within which the study area falls). It is intruded by anorogenic Jurassic Younger Granites in the Jos Plateau (Fig. 2.1).

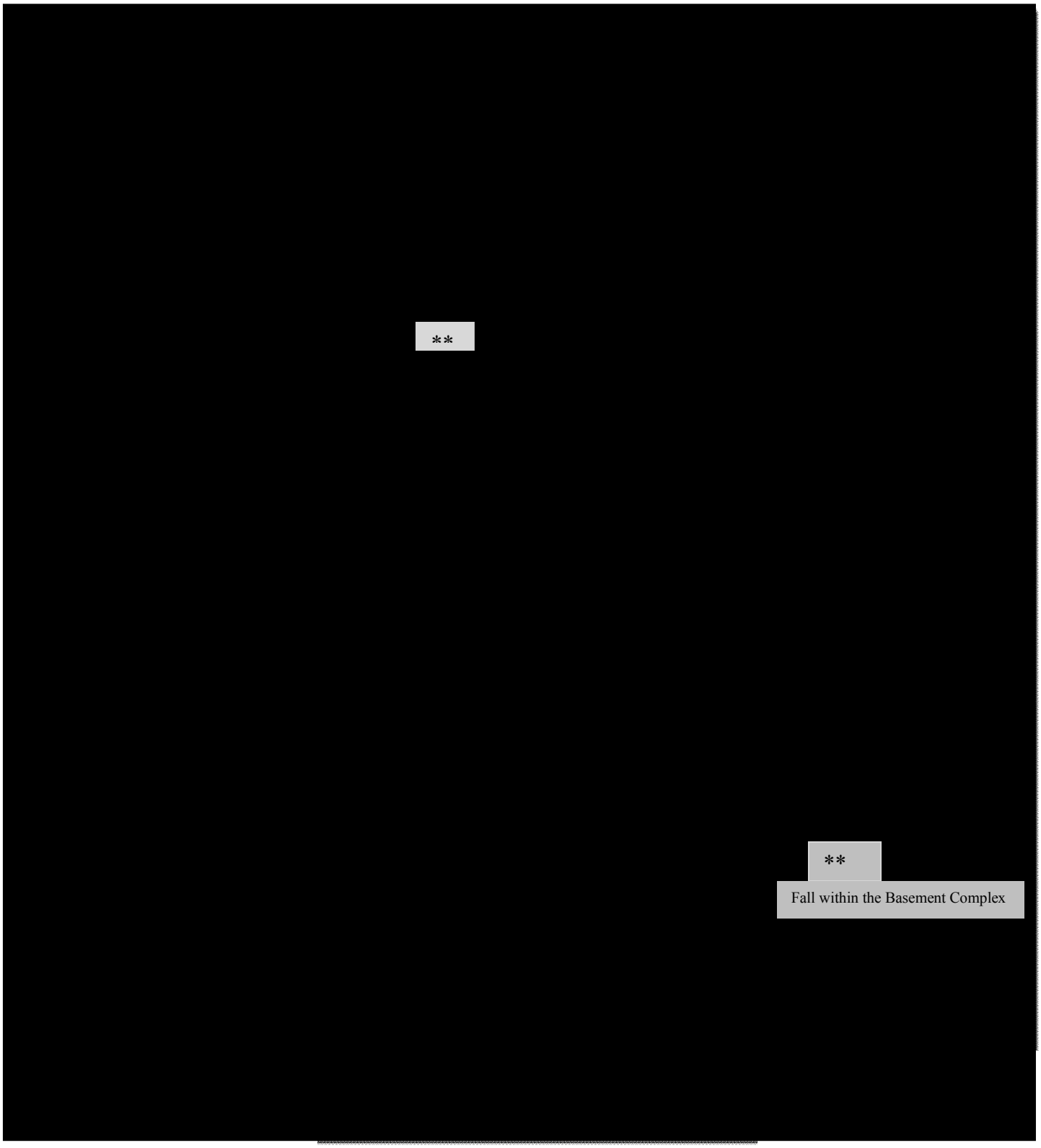



**FIG.2.1: OUTLINE GEOLOGICAL MAP OF NIGERIA (modified after Ajibade et.al, 1989)**

The Basement Complex has been affected by several cycles of tecto-metamorphic events. Based on radiometric dating, the Basement Complex has been affected by deformation involving thermal reactivation. Two of the Orogenic events have wide spread effect over the country; these are:

I The Eburnearn Orogeny (1950 ± 250 M.a) and

II The Pan-African Orogeny ( 600 M.a ).

During Orogenic events, large volumes of granite were emplaced and initial sedimentary rocks were thermally reactivated (Ajibade et al., 1988). Rocks of the Basement Complex show a general NW-SE and NE-SW structural trend, which seems to lie parallel to the limbs of major folds. Oyawoye (1972), Rahaman (1972, 1975) and McCurry (1976) have provided review dealing with the Basement Complex rocks of Nigeria.

The rocks of the Nigeria Basement Complex are grouped into three broad divisions;

I. Migmatite-Gneiss Complex,

II. Schist belts and

III. Older granites.

These are briefly discussed as follows.

**2.3.1 Migmatite-Gneiss Complex**

The Migmatite-Gneiss Complex is thought to have resulted from a complex association of deformative, shearing, folding, granitization and migmatisation processes. The slightly migmatized to unmigmatized paraschists represent a sedimentary cover on the Migmatite-Gneiss Complex. Rocks of the Migmatite-Gneiss Complex occupy most of the areas around Kano, Zaria, Funtua, Kaduna, Bauchi, Akwanga, Keffi, Abuja in the North; Ilorin, Ibadan, Ile-Ife in the West and around Obudu, the Oban Massifs and the Mamfe region in the South-East. This suite includes gneisses (banded, complexly deformed) and migmatites.

### 2.3.2 Schist Belts

Rocks of the schist belts occur predominantly in the Western half of Nigeria. Their lithologic compositon ranges from schists through phyllites to pelitic, semi-pelitic, and psammatic rocks as well as marble, quartzite and amphibolite (Obaje et al., 2006).

They generally occur in linear N-S trending belts which are more or less continuous for a distance of about 400 km along the strike. The belts are generally separated by Migmatite-Gneiss Complex and intruded by granitic rocks of the Older Granite suites. Occassional small isolated bands and lenses of the schist occur in the Migmatite-Gneiss Complex. The Schist belts have been studied in detail and mapped in Kazaure, Anka, Maru, Birnin Yauri, Birnin Gwari, Zungeru, Kushaka, Kushekiri, Igara, Ifon, Ilesha and Ile-Ife (Ajibade et al., 1989). In all these areas, they are known to be associated with commercial quantities of gold mineralization occurring in pegmatitic quartz veins.

The study area lies within the crystalline Basement Complex of the North-Western Nigeria and belongs to the Pan-African Older Granite suite. McCurry (1970) mapped 1200 $km^2$ area of Northern Nigeria which was later reviewed by Webb (1972).

### 2.3.3 The Older Granites

The Older Granites occur intricately associated with the Migmatite-Gneiss Complex into which they generally intrude. Older Granite rocks therefore occur in most places where rocks of the Migmatite-Gneiss Complex occur, but are particularly noteworthy in around Wusasa (Zaria), Abuja, Bauchi, Akwanga, Ibadan and Obudu.

Older Granite refers to rock series ranging in composition from Granite to Granodiorite (Oyawoye, 1964). Granite intrusion into the Nigeria basement occurred during the Eburnean and lower Cambrian ages. The Eburnean Granites are fine-grained Granites that represent a group of minor discordant intrusion of small aerial extent; occurring as dykes

and irregular bodies. The group include Biotite and Muscovite Granite and Adamelites. They are pale brown equigranular and usually foliated. Their contact with the later Granite is complex, but in some places degradational and in some places replaced by the later Granites. The most common types of Older Granites are:

I. Granodiorite Granite

II. Syenites Granite

III. Quartz-diorite Granite

IV. Porphyritic Biotite Granite

V. Fayalite quartz Monzolite and

VI. Aegerine Augen Granite

In the work of Eigbefo (1978) on Kubanni basin sheet 102, he listed the basement rocks found in the area as follows:

I. Coarse porphyritic-biotite Granite

II. Medium-Coarse grained biotite Granite-Gneiss

III. Apatite Granite; Pegmatites and Quartz veins intrude most of the bodies, and

VI. Weathered basement. This is about 14% of the basin's total area and forms a storage aquifer as he reported.

The surface of the Older Granite Basement in the study area was found to be overlain by a deposit which Wright and McCurry (1970) listed as Older laterite, Younger laterite, Older alluvium and Younger alluvium; the last two being Quaternary deposits. They added that the Older laterite is characterised by high topography, thickness of up to 7.00 metres, reddish-brown, cellular in nature and purer than the Younger laterite. The Younger laterite has lower topography, thickness is less than 6 meters, browner, and are mostly exposed along streams. The alluvia are formed almost at the same time with Younger laterite and are

seen everywhere in the area. They result in the accumulations of fine grey-brown sands, clays, red sand, silt and gravel to a thickness as much as 15 metres in some places.

Eigbefo (1978), noted that these surfacial deposits in the area did not only serve as a recharging medium to the aquifer but also as a storage when it is underlain by a weathered basement.

**2.4 Structural Geology of the Study Area**

Structural elements like faults, joints and fractures play important role in groundwater storage. They can control the flow rate, recharge and discharge modes of groundwater especially in the crystalline area as is the case in this study area. A prominent joint can store water especially when it is overlain by weathered basement. Akpoborie (1973), in a study on Kubanni basin, reported that the Older Granite inselbergs are intensively fractured giving way for easy recharge of weathered basement aquifer with rain water. Two major deformations were reported in his study of the area; the greater one is along N-S while a less prominent one is along E-W. These deformations are likely to arise in connection with the Nigeria Basement Complex faulting and fracture pattern caused by transcurrent movement. The deformations are oriented in the NW-SE and NE-SW directions (Oluyide and Udo, 1986).

The identified elements for groundwater storage in the study area from the various studies are weathered basement, Older laterite and alluvial deposits. The characteristics of these elements include- high porosity and permeability and less consolidation.

# CHAPTER THREE

# METHODOLOGY

## 3.1 Field-Work Planning

The field work was accomplished between 5th of October and 12th of October, 2009 shortly after the wet or rainy season. This period was chosen for the field work to avoid disturbances by the rain which would slow down the work.

The Vertical Electrical Sounding (VES) using Schlumberger array was used at forty (40) stations. A regular direction of N-S azimuth was maintained in the orientation of the profiles (fig 3.1).

### 3.1.1 Choice of Electrode Configuration

In order to achieve the aim and objective of this work, the Schlumberger array was chosen based on the following reasons:

I. In depth probing, the potential electrodes are fixed while only the current electrodes are moved symmetrically about the centre of spread. Thus, it is more convenient than Wenner array for sounding since only the two current electrodes are essentially moved. Although, practical difficulties in dragging several electrodes and long cables over rugged or wooded terrain is a slow and expensive task here.

II. The effect of shallow resistivity variation is constant with the fixed potential electrodes.

III. The electrode effect on the resistivity curve is greatly minimised (Kunetz, 1966; Parasnis, 1962).

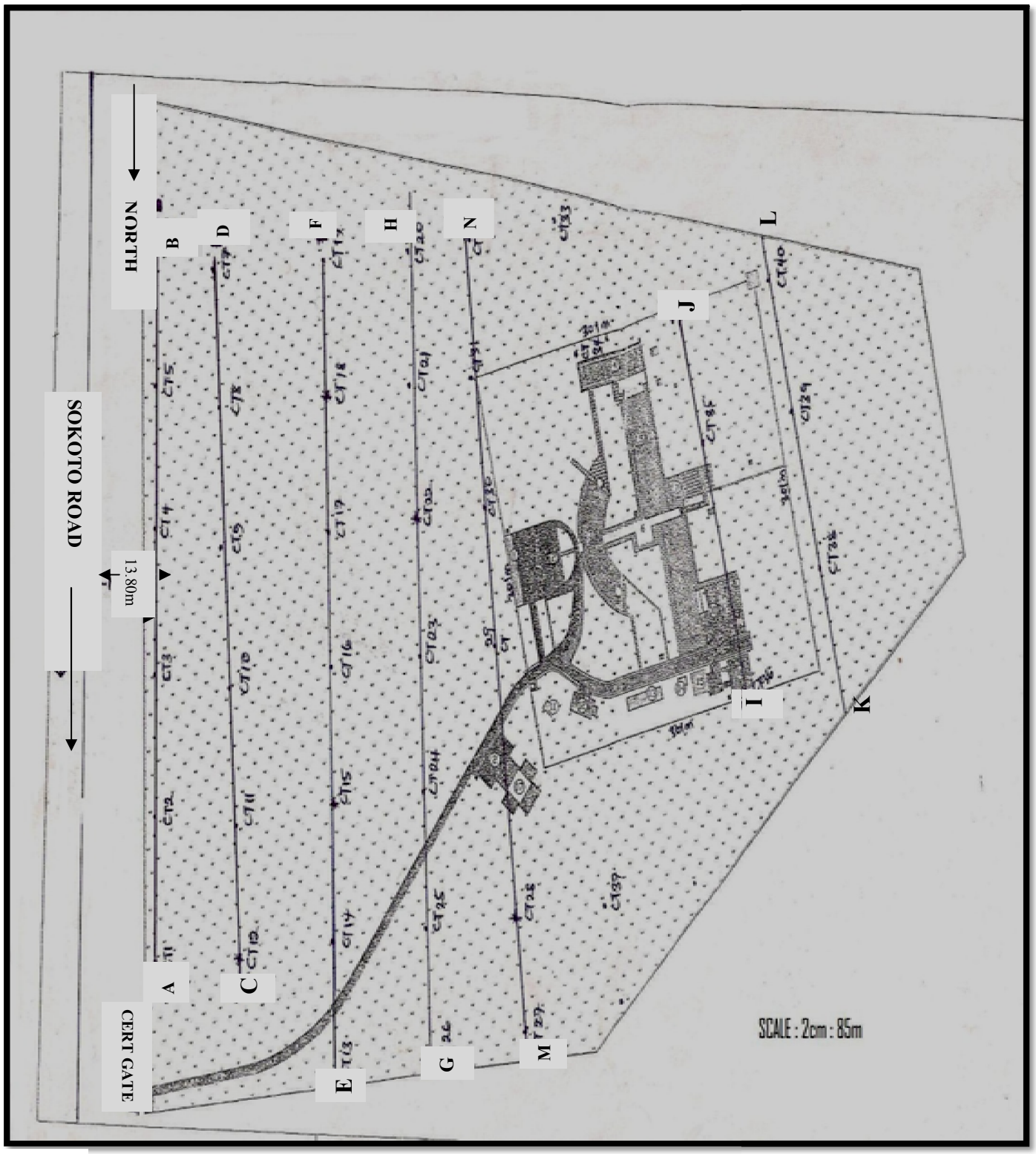



**FIG.3.1: VES STATIONS IN THE STUDY AREA.**

### 3.1.2 Resistivity Values of rocks and minerals

Of all the physical properties of rocks and minerals, electrical resistivity shows the greatest variation. While the range in density, elastic wave velocity and radioactive content is quite small, in magnetic susceptibility it may be as large as $10^5$. However, the resistivity of metallic minerals may be as small as $10^{-5}\Omega$m, that of dry, close grained rocks like gabbro as large as $10^7\Omega$m. The maximum possible range is even greater, from native silver ($1.6 \times 10^{-8}\Omega$m) to pure sulphur ($10^{16}\Omega$m).

The following geological and hydrogeological factors affect the resistivity of rocks and minerals:

**1. Mineral composition**: The common rock-forming minerals such as silicates, phosphates, carbonates, nitrates, sulphates, quartz, mica, feldspar, silicon e.t.c are poor conductors with resistivity greater than $10^7\Omega$m. The variation in the resistivity of minerals is quite large. Minerals like pyrrhotite and graphite are consistently good conductors while pyrite, galena and magnetite are poor conductors in bulk form, although the individual crystals have high conductivity. Hematites and sphalerite, in pure form, are practically insulators, but when combined with impurities may have resistivities as low as $0.1\Omega$m. Graphite is often the connecting link in mineral zones which makes them good conductors

Very roughly, igneous rocks have the highest resistivity, sediments the lowest, with metamorphic rocks intermediate. However, there is considerable overlapping, as in other physical properties. In addition, the resistivities of particular rock types vary directly with age and lithology, since the porosity of the rock and salinity of the contained water affected

by both. For example, the resistivity range of Precambrian volcanics is 200 - 5000Ωm, while for Quaternary rocks of the same kind it is 10 - 200Ωm.

**2. Porosity and degree of water saturation**: The resistivity of sub-surface rock is greatly affected by the presence of groundwater. The minerals which form the matrix of a rock are generally poorer conductors than the groundwater and hence the effective resistivity of the rock is decreased by the groundwater. Hence, a small change in the percentage of the water content affects resistivity of the earth materials significantly. Increasing the amount of water decreases the resistivity of a water bearing rock.

Porosity = (total volume of pore spaces / total volume of rock) x 100% *(3.1)*

Igneous and Metamorphic rocks usually have low porosity unless they are fractured while sedimentary rocks usually have high porosity. Usually, the higher the porosity the lower the rock resistivity.

**3. Mineralization of the water content of pore spaces**: Rock resistivity vary with the salt contents of the water in the pore spaces with the result that the greater the amount of the dissolved salts the lower the resistivity. Conduction in near surface rock is almost entirely through the water content in the pore spaces i.e. electrolytic conduction.

**4. Temperature effect**: Extreme temperature ranges greatly affect the resistivity of water bearing rocks. Particularly if the temperature is high enough to expel the water in the rock as steam or low enough to freeze the water. At moderate temperature, rock resistivities usually decreases with increasing temperature. i.e rocks have negative temperature coefficient of resistivity. Metals have positive temperature coefficient i.e their resistivity increases with increasing temperature. Since the mobility of the electrons decreases with

increasing temperature. Since the number of conduction electrons in a semi-conductor of resistivity is usually negative.

However, increasing temperature decreases the mobility of electrons and this may more than offset the effect of an increased number of conduction electrons. Thus, semi-conductors may have a negative temperature coefficient of resistivity at the low portion of the temperature range and positive coefficient at the higher portion of the temperature range.

**5. Structure and texture of rocks**: Well sorted rocks usually have high resistivities while poorly sorted rocks are usually have low resistivities. The texture of a rock also affects resistivity. Usually the finer the rock grain size the lower the resistivity.

The geometrical arrangement of the interctices in the rock has less pronounced effect, but may make the resistivity anisotropic, that is, having different magnitudes for current flow in different directions. Anisotropy is the characteristic of stratified rock which is generally more conductive in the bedding plane. The anisotropy coefficient, which is the ratio of the maximum to minimum resistivity, may be as large as two in some graphitic slates and varies from 1 to 1.2 in some rocks such as limestone, shale and rhyolite.

As an example, in considering a layered formation, having resistivities $\rho_1$ and $\rho_2$ whose respective fractional volumes are $V$ and $1 - V$. Here the resistivity in the horizontal direction – a stack of beds effectively in parallel is

$$\rho_h = \rho_1\rho_2 / \{\rho(1 - V) + \rho_2 V\}; \qquad (3.2)$$

In vertical direction, the beds are in series so that

$$\rho_v = \rho_1 V + \rho_2(1 - V). \qquad (3.3)$$

Then the ratio is

$$\rho_h / \rho_v = (1 - 2V + 2V^2) + (\rho_1/\rho_2 + \rho_2/\rho_1)\, V\,(1 - V). \qquad (3.4)$$

If V is much less than 1 and $\rho_2/\rho_1$ is much greater than 1, this simplifies to

$$\rho_V / \rho_h \approx 1 + (\rho_2/\rho_1)V. \qquad (3.5)$$

If the layer of the resistivity $\rho_1$, is for water- saturated beds, this ratio might be quite large.

Table 4.2 and 4.3 respectively show the resistivity values of the rock types in Basement Complex areas similar to the study area, compiled from (Telford et al., 1976, 1990). Table 4.4 shows similar values that were adopted for the interpretation of the VES data.

**3.1.3 Electrical Properties of Earth materials and Parameters.**

The electrical parameters of properties of rocks and minerals exploited in the electrical prospecting are; electrical conductivity or its inverse electrical resistivity, natural electrical potentials, dielectric constant and magnetic permeability.

The most important of these parameters is the conductivity. Electrical current flow in earth's material is determined to a large extent by the medium's resistivity and to a lesser extent by the dielectric constant and magnetic permeability.

**3.1.3.1 Electrical Conductivities**

Electric current may be propagated in rocks and minerals in three ways: electronic (ohmic), electrolytic and dielectric conduction. The first is the normal type of current flow in materials containing free electrons, such as the metals. In an electrolyte the current is carried by ions at a comparatively slow rate. Dielectric conduction takes place in poor conductors or insulators, which have very few free carriers or none at all. under the influence of an external varying electric field, the atomic electrons are displaced slightly with respect to their nuclei; this slight relative separation of negative and positive charges is known as dielectric polarization of the material. Ionic and molecular polarization may

occur in materials with ionic and molecular bonds. In all these cases dielectric conduction is the result of changing electronic, ionic or molecular polarization caused by the alternating electric field.

**1. Electronic Conduction**: The electrical resistivity of a cylindrical solid of length *L* and cross-section *A*, having resistance *R* between the end faces, is given by

$$\rho = RA/L. \qquad (3.6)$$

If *A* is in meters$^2$, *L* in meters and *R* in ohms, the resistivity unit is the ohm-metre (Ωm). The resistance *R* is given in terms of the voltage *V* applied across the ends of the cylinder and the resultant current in *I* flowing through it, by Ohm's law:

$$R = V/I, \qquad (3.7)$$

where *R* is in ohms and the units of *V* and *I* are volts and amperes.

The reciprocal of resistivity is the conductivity σ, the units being mhos/m or mhos/cm. The

$$\sigma = 1/\rho = L/RA = (I/A)\ (V/L) = j/E \qquad (3.8)$$

Where *j* = current density (amperes/m$^2$), *E* = electric field (volts/m).

**2. Electrolytic Conduction:** Since most rocks are poor conductors, their resistivities would be extremely large were it not for the fact that they are usually porous and the pores filled with fluid, mainly water. As a result the rocks are electrolytic conductors, whose effective resistivity may be define as in

$$\rho = RA/L. \qquad (3.9)$$

But it must be kept in mind that the conduction is electrolytic rather than ohmic. That is, the propagation of current is by ionic conduction- by molecules having an excess or deffiency of electrons. Hence the resistivity varies with the mobility, concentration and degree of dissociation of the ions; the latter depends on the dielectric constant of the solvent. As

mentioned previously the current flow is slow compared to ohmic conduction and the movement represents an actual transport of material, usually resulting in chemical transformation.

The conductivity of a porous rock varies with the volume and arrangement of the pores and even more with the conductivity and amount of contained water. According to the empirical formula due to Archie (1942),

$$\rho = a\phi^{-m}S^{-n}\rho_w, \qquad (3.10)$$

Where $\phi$ = fractional pore volume (porosity), s = fraction of the pores containing water, $\rho_w$ = resistivity of water, $n \approx 2$, a,m = constants, $0.5 \leq a \leq 2.5$, $1.3 \leq m \leq 2.5$.

Water conductivity varies considerably in the range of 0.05 to 3 x $10^3$, depending on the amount and conductivity of dissolved chlorides, sulphates and other minerals present.

Electronic conduction mechanisms are more important than the electrolytic conduction mechanisms through pore water in the following three cases;

I. In rocks containing a high percentage of conducting minerals such magnetite, graphite or pyrrhotite.

II. In rocks which are completely frozen.

III. In rocks which lie sufficiently deep in the earth so that all the pore spaces are closed by overburden pressure.

**3. Dielectric Conduction:** The mechanism of dielectric conduction – the displacement current flows only in non-conductors when the external electric field changes with time. The significant parameter in dielectric conduction is the dielectric constant, *k*, sometimes called the specific inductive capacity of the medium.

The dielectric constant is similar to the conductivity in porous formations in that it varies with the amount of water present (water has a very large dielectric constant ≈ 80 kHz at low frequency).

**3.1.3.2 Electrical potentials**

Certain natural or spontaneous potentials occurring in the subsurface are caused by electrochemical or mechanical activity. The controlling factor in all cases is the underground water. These potentials are associated with weathering of sulphide mineral bodies, variation in rock properties (mineral content) at geologic contacts, bioelectric activity of organic material, corrosion, thermal and pressure gradients in underground fluids and other phenomena of similar nature. There are four principal mechanisms producing these potentials; the first is mechanical, the latter three chemical, in origin.

**1. Electrokinetic potential**; Also known as streaming potential, this is a well known effect observed when a solution of electrical resistivity ρ and viscocity η if forced through a capillary or porous medium. The resultant potential difference between the ends is

$$E_k = -\phi \Delta P \varepsilon \rho / (4 \quad \eta) \qquad (3.11)$$

Where ϕ = adsorption (zeta) potential, ΔP = pressure difference, ε = solution dielectric constant.

The quantity ϕ is the potential of a double layer (solid-liquid) between the solid and solution. Although generally of minor importance, the streaming effect may be the cause of occasional large anomalies associated with topography. It is also observed in self-potential well logging, where the drilling fluid penetrates porous formations.

**2. Liquid-junction (diffusion) potential**; This is due to the difference in mobilities of various ions in solutions of different concentrations. The value is given by

$$E_d = - R \quad (I_a - I_c) / \{F_n(I_a + I_c) \log (C_1/C_2)\} \qquad (3.12)$$

($E_d$ being in millivolts).

*W*here $R$ = gas constant (8.31 joules/°C), $F$ = Faraday constant (9.65 x $10^4$ C/mol), = absolute temperature, $n$ = valence, $I_a$ and $I_c$ = mobilities of anions and cations, $C_1$ and $C_2$ = solution concentrations.

**3. Shale (Nernst) potential**: When two identical metal electrodes are immersed in homogeneous solution, there is no potential difference between them. If, however, the concentrations at the two electrodes are different, there is a potential difference given by

$$E_s = R \quad / F_n \log (C_1/C_2) \qquad (3.13)$$

(*Es* in millivolts)

The combined diffusion and Nernst potentials are known as the electrochemical or static, self-potential.

**4. Mineralization potential**: When two dissimilar metal electrodes are immersed in homogeneous solution, a potential difference exists between the electrodes. This electrolytic contact potential, along with the static self-potential, is undoubtedly among the basic causes of the large potentials associated with certain minerals zones and known as mineralization potentials. These potentials, which are especially pronounced in zones containing sulphides, graphite and magnetite, are much larger. Values of several hundred millivolts are common and potentials greater than one volt have been observed in zones of graphite and alunite. Because of the large magnitude, mineralization potentials cannot be attributed solely to the electrochemical potentials earlier. The presence of metallic

conductors in appreciable concentrations appears to be necessary condition; nevertheless, the exact mechanism is not entirely clear.

### 3.1.3.3 Dielectric constants of rocks and minerals

The dielectric constant is a measure of the electrical polarization resulting from an applied electric field. The polarization may be electronic, ionic or molecular. The electronic is characteristic of all non-conductors. Ionic displacement occurs in many rock-forming minerals, while water and the hydrocarbons are only common materials which exhibit molecular polarization. Because of the relatively slow mobilities of the charge carriers, molecular polarization – the largest of the three effects – and ionic polarization are insignificant at very high frequencies. Thus the dielectric constant, which is proportional to the degree of polarization, varies inversely with frequency. It is also indicative of the amount of water present, since water has a dielectric constant of 80 at low frequencies.

### 3.1.3.4 Magnetic permeability

This property of earth materials has only a slight effect on the electrical measurement except there is a large fraction of a ferro-magnetic materials (concentrated magnetite, pyrrhotite and ilmenite) present. Magnetic permeability $\mu$ is related to magnetic susceptibility $k$ by the following relation;k

$$\mu = 1 + 4\ k \text{ in cgs units,} \qquad (3.14)$$

$$\mu/\mu_0 = 1 + K \text{ in MKS units.} \qquad (3.15)$$

Generally, magnetic susceptibility $K$ is very small so, that the above ratio is not appreciably different from unity.

### 3.1.4 Data Collection

The choice of the sounding location was made so as to cover the whole area in order to achieve the set objectives. At each VES point, N-S azimuth was taken along the profile.

Previous geophysical work, carried out within the northern part of Nigeria, has shown that the overburden in the basement area is not as thick as to warrant large current electrode spacing for deeper penetration (Oyawoye, 1964). Therefore the largest current electrode separation AB used was 200m, that is, 1/2AB = 100m.

According to Barker (1989), the maximum depth of penetration in Shlumberger array is 0.19AB, 0.175AB for Wenner array and 0.245AB for dipole-dipole array. The potential electrode separation, MN, is usually increased intermittently in order to maintain a measurable potential, but this increase should not exceed one-fifth of the half-current electrode separation, 1/2AB, as suggested by Dobrin and Savit (1988).

### 3.1.5 Instrumentation

The principal instrument used for this survey was the ABEM terrameter Signal Averaging System (SAS) 300. No booster was used because the expected depth-to-basement in the area is within the range of penetration of instrument. The resistance reading at every point was automatically displayed on its digital read out screen and was written down. The SAS 300 can operate in two modes:

I. Resistivity Survey mode: It contains a resistivity meter, suitable for current electrode spacing of up to 2000m under good surveying conditions. The change in potential difference per unit current ($\Delta V/I$) is automatically calculated and displayed in digital form (in ohms or milli-ohms). The overall range is from 0.5 milli-ohm to 1999 kilo-ohms. This mode was chosen for this work. However, the range can be extended down to 0.02 milli-ohm by means of the SAS 300 Booster, but this was not necessary for this survey.

II. Voltage measuring mode: The SAS 300 comprises a self potential instrument that measures natural d.c. potentials. The result is displayed in volts or milli volts. The overall range extends from 0.01mV to 500V.

### 3.2 Basis and Theory of the Method used

#### 3.2.1 Basis of D.C. Resistivity Method

This method is based on the fact that when an electric current is driven into the earth, any variation of the subsurface resistivity will alter the current flow, which will in turn affect the distribution of the electric potential. The measurement of the electrical potential and current on the earth's surface will make it possible to obtain information about the resistivity variation of the subsurface in the area concerned (Telford et al., 1976).

The regular pattern of current flow will be distorted by buried bodies or geological structures. For instance a conductive body will concentrate the electric current flow lines towards itself, while a resistive body will cause the current to flow round it and less concentrated in it. The potential fields are hence deflected; the deflections can be observed by the potential electrodes at the surface of the earth. The ratio of potential difference to the electric current applied gives the resistance from which resistivity of the target subsurface body can be obtained.

#### 3.2.2 Theory of D.C. Resistivity Method

Shlumberger array, Fig. 3.2 was adopted for the survey. A and B are point current electrodes through which current is driven into the ground, while M and N are two potential electrodes to record the potential distribution in the subsurface within the two current electrodes.

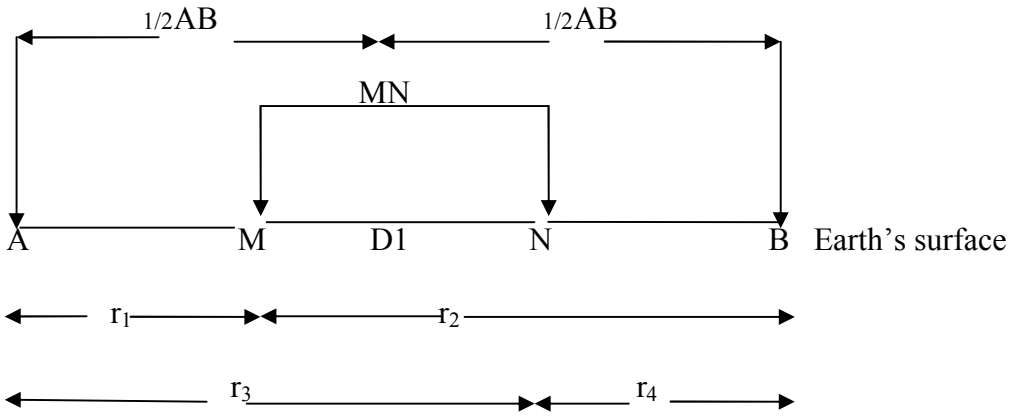



**Fig. 3.2: Shlumberger array**

From Ohm's law, the current I and potential V in a metal conductor at constant temperature are related as follows:

$$V = IR \qquad (3.17)$$

where R is the constant of proportionality termed resistance and it is measured in ohms. The resistance R, of a conductor is related to its length L and cross sectional area A by;

$$R = \rho L / A \qquad (3.18)$$

where ρ is the resistivity and it is a property of the material considered.

From equation (1) and (2),

$$V = I\rho L / A \qquad (3.19)$$

The vertical electrical sounding (VES) with Schlumberger array involves fixing the potential electrodes at point M and N, and symmetrically increasing the current electrode separation AB about the centre by displacing A and B outwardly in steps. This will increase the depth of penetration within the separation AB. Thus the varying resistivity measured when electrode array position is varied in an inhomogeneous medium is termed apparent resistivity.

For simple treatment, a semi-infinite solid with uniform resistivity, ρ, is considered. A potential gradient is measured at M and N when current electrodes located on the surface of the equipotential surface is semi-spheral downward into the ground at each electrode. The surface area will then be $2\pi L^2$, where L is the radius of the sphere. Thus

$$V = I\rho / 2\pi L \qquad (3.20)$$

By deduction then, the potential at M ($V_M$), due to the two current electrodes, is

$$V_M = I\rho/\{2\pi\,(1/r_1 - 1/r_2)\} \qquad (3.21)$$

Similarly, the potential at electrode N ($V_N$) is given by

$V_N = I\rho/\{2\pi\ (1/r_3 - 1/r_4)\}$ *(3.22)*

where $r_1$, $r_2$, $r_3$ and $r_4$ are shown in figure 3.2.

The potential difference, $\Delta V$, across electrodes M and N is $V_M - V_N$. If the body is inhomogeneous like the study area, apparent resistivity ($\rho_a$) is considered,

$\rho_a = K\ (\Delta V/\ I)$ *(3.23)*

Where $\rho_a$ is apparent resistivity in ohm-metre, and

$K = 2\pi\ [(1/r_1 - 1/r_2) - (1/r_3 - 1/r_4)]^{-1}$ *(3.24)*

K is called the geometric factor whose value depends on the type of electrode array used.

For Schlumberger array, if MN =2b and 1/2AB = L then,

$K = \pi\ (L^2/2b - b/2)$ *(3.25)*

**3.3 Data Reduction**

Equation (3.23) was used to obtain apparent resistivity values for each point. To do this, the geometric factors, K, are first calculated for all the current electrode spacings using equation (3.25). The values obtained, were then multiplied with the resistance values got from the field data. Then the apparent resistivity, $\rho_a$, values for each point were plotted against the electrodes spacing (1/2AB) on a log-log graph to obtain the model, field and synthetic curves using an appropriate computer software (IPI2win).

The azitmuthal data were similarly reduced and a linear plot was obtained for the apparent resistivity, $\rho_a$, versus the electrode spacing (1/2 AB) along each of the four azimuths i.e N-S, E-W, NE-SW and NW-SE. Thus, resistivity anisotropies and geological deformational trends were observed from the plots in figure 4.13.

### 3.4 IPI2win Model overview

IPI2win is designed for automated and interactive semi-automated interpretation of vertical electric sounding or induced polarization data obtained with any of a variety of the most popular arrays used in electrical prospecting. It is presumed that a user is an experienced interpreter willing to solve the geological problem posed as well as to fit the sounding curves.

#### 3.4.1 Data Managing

To start the process of interpreting IPI2win, there is need for a data file of certain format containing the information on the measurement system and apparent resistivity (and apparent chargeability in the VES-IP mode) values for desegmented curves (*.dat) or for segmented curves (*.dtg). A dtg-file may also contain potential difference and electric current values for schlumberger and half-schlumberger arrays.

**1. Entering data**: The dgt-file is generally created using the external text editor (i.e windows Notepad). IPI2win internal utility for creating data file is run by choosing the file, New VES point menu item, or by clicking the (make New VES point) button in the tool bar, or by pressing the [ctrl - Alt- N] key. The New VES point window will appear. The apparent resistivity curve (VES-IP mode – and apparent resistivity curve) is displayed in the right part of the window. The left part of the window is a table of field data, each line represents spacing. The columns of the table are spacings (AB/2 column), measurement line length (MN), apparent chargeability (SP), voltage (U), current (I), coefficient (K), apparent resistivity (Ro_a). Spacing and measurement line length must be typed into the correspondent cells of the table. To enter apparent resistivity, click the input apparent resistivity button window, then type the values in the corresponding cells. When editing the table, one can use the copy and paste buttons of the window.

The table contents can be stored in the clip board by clicking the (copy table) button of the window. The stored items can be pasted then into a spreadsheet or word processor. The table contents can also be saved as the text file by clicking the (save Txt) button of the window. The array type must be selected from the array drop-down list of the window. After all the data are entered, click the (add) button of the window to append to curve to the currently opened file or the (ok) button of the window to start creation of the new data file. In any case, save as… window will be displayed, where the file name must be pointed out or typed in the file name text box.

**2. Viewing Curves and Models**: The sounding curve for a certain point is displayed in the curve window titled with the sounding point name. The point name is duplicated in the name of VES location field of the status line immediately below the toolbar. Only one curve can be displayed at a time. The position of the sounding point on the profile is marked by a vertical line on the cross-sections in the cross-sections window.

The field values of the apparent resistivity are marked by circles. The curve itself is presented by a black line, which is a smoothing spline on the field values. The curve is plotted in the algorithmic scale for both spacing and apparent resistivity axes. The number of the orders on either of the axes is determined automatically, so the scale of the curve plot may vary at the different sounding points.

**3. Interpreting Sounding data**: The concept of the profile interpreting is the foundation of IPI2win. It means that data for a profile are treated as a unity representing the geological structure of the survey area as a whole, rather than a set of independent objects dealt seperately. The concept is implemented mainly by using the semi-interactive mode rather than the automated interpreting model.

IPI2win is capable of solving resistivity electrical prospecting 1D forward and inverse problems for a variety of commonly used arrays for the cross-sections with resistivity contrasts within 0.001 to 10000. The forward problem is solved using linear filtering. The filters are developed at the near surface Electrical Prospecting Lab, Geophysical dept., Geological Faculty, Moscow State University, Moscow, Russia. The thoroughly tested filters and filtering algorithm implementation provide fast and accurate direct problem solution for a wide range of models, covering all reasonable geological situations.

**4. Discarding Changes**: Any completed editing operation can be discarded by pressing the [Alt-Backspace] keys, choosing the Edit, Undo menu item or clicking the (Undo) button on the toolbar. The editing operation is completed when the [Enter] key is pressed after typing a value in the cell of the table in the model window or the mouse button is released after dragging the pseudo-log plot segment.

**5. Clearing Model**: Sometimes it is necessary to delete the model for a certain point, i.e. to start interpreting from the very beginning. To do this, select the point with the desired model and choose the Edit, Cut model menu item, or press [shift-Del] keys, or click the [Cut] button on the toolbar. To clear the models for the points, currently displayed in the cross-section window, choose the Delete all results menu item.

# CHAPTER FOUR

# INTERPRETATION OF RESULTS AND DEDUCTIONS

## 4.1 General Statement

The interpretation of Vertical Electrical Sounding (VES) data involves expressing the information obtained from the surface measurements in geological terms. In doing so, the combination of some subsurface structural parameters like resistivities and layer thicknesses are obtained.

For easy interpretation, it is assumed that:

1. The various geoelectric layers encountered are electrically homogenous or uniform and isotropic. However, lateral variation in resistivity exists within a geoelectric layer. Therefore, any deviation from this ideal situation adds to the error in the final interpretation (Kearey and Brooks, 1984).

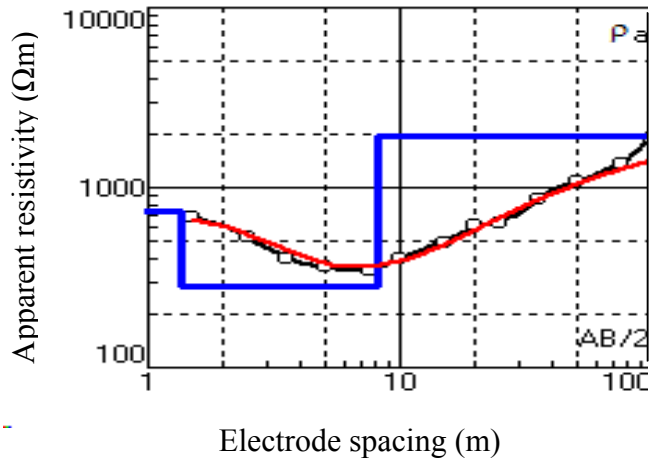
2. The computed resistivity curves are based on the fact that the subsurface layers are horizontal and unique. This may not be true in all cases especially in a case of vertical contact. Thus, any vertical layer boundary encountered will introduce error into the interpretation.

3. Each subsurface layer is unique as regards its curve. However, the interpretation suffers from non-uniqueness arising from problems of equivalence and suppression (Kunetz, 1966). From Kunetz, the problem of equivalence is the difficulty in distinguishing between two resistive layers of different thicknesses and resistivities where product of these parameters are the same. Similarly, two layers may not be distinguished if the ratio of their thickness to resistivity is the same. The problem of suppression is associated with those

layers whose resistivities are intermediate between the resistivities of the enclosing layers. Such layers (with small thicknesses) will have no practical influence on the VES curves.

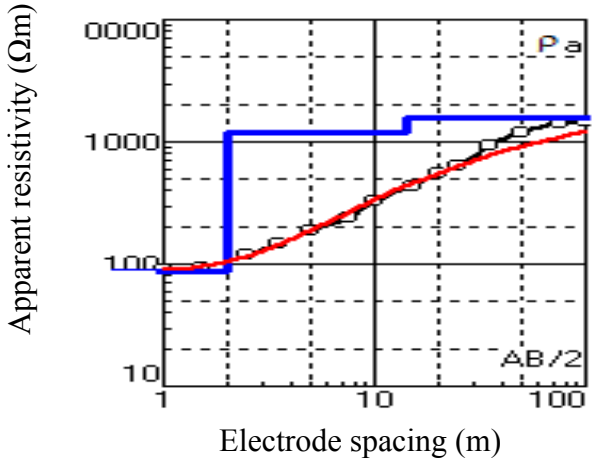
### 4.1.1 Interpretation

The field data obtained have been analysed using a computer software (IPI2win) which gives an automatic interpretation of the apparent resistivity data. Figures 4.1, 4.2, 4.3, 4.4 and 4.5 are examples of curve types and models obtained from VES stations CT 1, CT 3, CT 5, CT 10 and CT 34. Similar plots and interpreted models were obtained for each of the 40 VES points shown in Appendix 1. Table 4.1 shows the results of the interpreted VES curves.



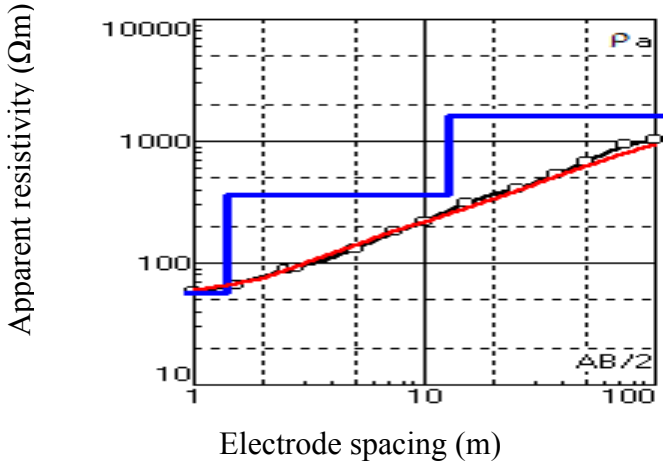

| N | ρ | h | d |
|---|---|---|---|
| 1 | 738 | 1.35 | 1.35 |
| 2 | 282 | 6.81 | 8.16 |
| 3 | 1931 | | |
| | | | |

FIGURE 4.1: VES CURVE AT STATION CT1 (TYPE H).



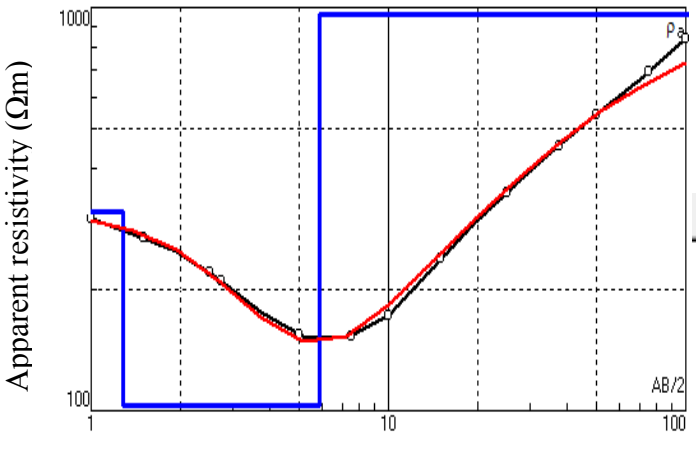

| N | ρ | h | d |
|---|---|---|---|
| 1 | 87 | 2.11 | 2.11 |
| 2 | 1179 | 12.30 | 14.4 |
| 3 | 1585 | | |
| | | | |

FIGURE 4.2: VES CURVE AT STATION CT3 (TYPE A)



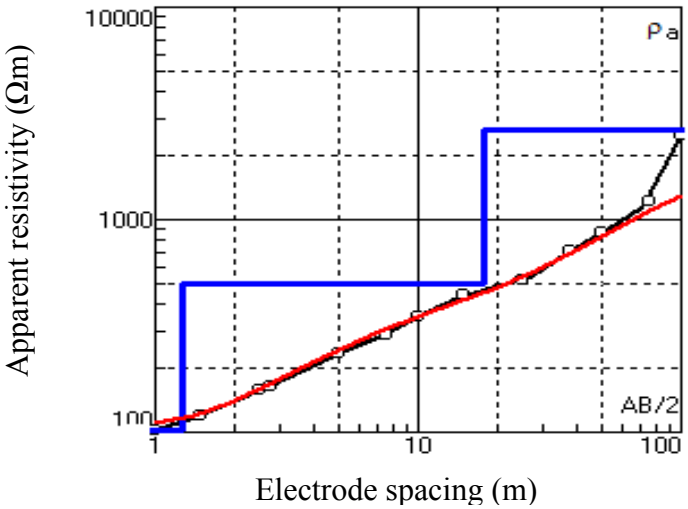

| N | ρ | h | d |
|---|---|---|---|
| 1 | 57 | 1.37 | 1.37 |
| 2 | 326 | 11.4 | 12.77 |
| 3 | 1630 | | |
| | | | |

FIGURE 4.3: VES CURVE AT STATION CT5 (TYPE A).




| N | ρ | h | d |
|---|---|---|---|
| 1 | 300 | 1.28 | 1.28 |
| 2 | 119 | 4.65 | 5.93 |
| 3 | 990 | | |
| | | | |

FIGURE 4.4: VES CURVE AT STATION CT10 (TYPE H).




| N | ρ | h | d |
|---|---|---|---|
| 1 | 108 | 1.21 | 1.21 |
| 2 | 546 | 9.42 | 10.63 |
| 3 | 2859 | | |
| | | | |

FIGURE 4.5: VES CURVE AT STATION CT34 (TYPE A)

Where

**N** is the layer number,

**ρ** is the layer resistivity in (Ωm)

**h** is the layer thickness in metres and

**d** is interface depth in metres.

The interpretation of these curves was based on the principle that all points of maxima and minima are indicators of different lithologies. Similarly, where the resistivity values tend to infinity is an indication of the fresh basement rock (Telford et al., 1976, 1990).

In addition, in order to help see at a glance the resistivity distributions over the whole area, comprehensive subsurface isoresistivity contours at various points at preferred depth were produced. Conversely, depth contours were plotted at various predetermined resistivity values using a computer software (Sufer 7.0 model).

Remarkable geologic deformational trends were observed on the azimuthal VES plots (figure 4.13). A linear plot was obtained for apparent resistivity, $\rho_a$, values plotted against the electrode spread (1/2AB) along each of the four azimuths (i.e. N - S, E - W, NE - SW and NW - SE). The presence of the subsurface anisotropy sometimes depicts occurrence of structural elements like fractures, faults, cracks or fissures (Telford et al., 1976, 1990), whose presence in a water bearing bed can serve as groundwater storage.

**Table 4.1: THE RESULTS OF THE INTERPRETED VES CURVES.**

| Stations | Layer Thickness (m) | Layer resistivity (Ωm) | Remarks | Curve types | Number of layers |
|---|---|---|---|---|---|
| CT1 | 1.35<br>6.81<br>- | 738<br>282<br>1931 | TP<br>WB<br>FB | H | 3 |
| CT2 | 1.19<br>6.77<br>- | 738<br>312<br>1835 | TP<br>WB<br>FB | H | 3 |
| CT3 | 2.11<br>12.30<br>- | 87<br>460<br>1585 | TP<br>WB<br>FB | A | 3 |

| | | | | | |
|---|---|---|---|---|---|
| CT4 | 2.89<br>2.24<br>- | 63<br>150<br>960 | TP<br>WB<br>FB | A | 3 |
| CT5 | 1.37<br>11.40<br>- | 57<br>326<br>1630 | TP<br>WB<br>FB | A | 3 |
| CT6 | 3.90<br>6.20<br>- | 376<br>105<br>980 | TB<br>WB<br>FB | H | 3 |
| CT7 | 1.26<br>3.20<br>- | 18<br>757<br>927 | TP<br>WB<br>FB | A | 3 |
| CT8 | 1.36<br>0.78<br>- | 97<br>287<br>3162 | TP<br>WB<br>FB | A | 3 |
| CT9 | 1.23<br>0.52<br>- | 93<br>287<br>3054 | TP<br>WB<br>FB | A | 3 |
| CT10 | 1.28<br>4.65<br>- | 300<br>119<br>990 | TP<br>WB<br>FB | H | 3 |
| CT11 | 1.26<br>4.06<br>- | 296<br>185<br>1000 | TP<br>WB<br>FB | H | 3 |
| CT12 | 1.18<br>4.08<br>- | 91<br>321<br>1134 | TP<br>WB<br>FB | A | 3 |
| CT13 | 2.48<br>- | 9<br>534 | WB<br>FB | | 2 |
| CT14 | 2.42<br>2.76<br>- | 135<br>618<br>2364 | TP<br>WB<br>FB | A | 3 |
| CT15 | 2.85<br>6.86<br>- | 87<br>197<br>1230 | TP<br>WB<br>FB | A | 3 |
| CT16 | 1.21<br>9.42<br>- | 108<br>546<br>2859 | TP<br>WB<br>FB | A | 3 |

| | | | | | |
|---|---|---|---|---|---|
| CT17 | 1.23<br>9.49<br>- | 107<br>404<br>2783 | TP<br>WB<br>FB | A | 3 |
| CT18 | 1.95<br>7.94<br>- | 118<br>501<br>1540 | TP<br>WB<br>FB | A | 3 |
| CT19 | 1.94<br>4.34<br>- | 125<br>735<br>3574 | TP<br>WB<br>FB | A | 3 |
| CT20 | 1.36<br>8.65<br>- | 55<br>116<br>1072 | TB<br>WB<br>FB | A | 3 |
| CT21 | 1.96<br>2.68<br>- | 132<br>313<br>2257 | TP<br>WB<br>FB | A | 3 |
| CT22 | 2.40<br>4.61<br>- | 112<br>442<br>1610 | TP<br>WB<br>FB | A | 3 |
| CT23 | 3.35<br>10.10<br>- | 320<br>236<br>1110 | TP<br>WB<br>FB | H | 3 |
| CT24 | 2.08<br>5.23 | 121<br>97<br>944 | TP<br>WB<br>FB | H | 3 |
| CT25 | 1.63<br>8.08<br>- | 20<br>170<br>990 | TP<br>WB<br>FB | A | 3 |
| CT26 | 1.97<br>6.12<br>- | 50<br>249<br>1011 | TB<br>WB<br>FB | A | 3 |
| CT27 | 1.69<br>0.60<br>- | 104<br>229<br>6036 | TP<br>WB<br>FB | A | 3 |
| CT28 | 1.69<br>7.32<br>- | 32<br>933<br>1322 | TP<br>WB<br>FB | A | 3 |
| CT29 | 1.30<br>19.50<br>- | 96<br>588<br>1277 | TP<br>WB<br>FB | A | 3 |
| CT30 | 1.94<br>4.34<br>- | 123<br>987<br>2584 | TP<br>WB<br>FB | A | 3 |
| CT31 | 1.36<br>8.64 | 55<br>116 | TB<br>WB | A | 3 |

| | | | | | |
|---|---|---|---|---|---|
| | - | 1072 | FB | | |
| CT32 | 1.37<br>2.67<br>- | 8<br>336<br>990 | TP<br>WB<br>FB | A | 3 |
| CT33 | 1.57<br>9.04<br>- | 14<br>275<br>1369 | TP<br>WB<br>FB | A | 3 |
| CT34 | 1.21<br>9.42<br>- | 108<br>546<br>2857 | TP<br>WB<br>FB | A | 3 |
| CT35 | 3.91<br>23.00<br>- | 336<br>159<br>991 | TP<br>WB<br>FB | H | 3 |
| CT36 | 2.01<br>20.50<br>- | 61<br>613<br>1026 | TB<br>WB<br>FB | A | 3 |
| CT37 | 2.08<br>8.83<br>- | 49<br>966<br>3162 | TP<br>WB<br>FB | A | 3 |
| CT38 | 1.72<br>3.43<br>- | 43<br>248<br>1150 | TP<br>WB<br>FB | A | 3 |
| CT39 | 1.22<br>10.70<br>- | 13<br>158<br>961 | TB<br>WB<br>FB | A | 3 |
| CT40 | 2.24<br>10.60<br>- | 24<br>681<br>1150 | TP<br>WB<br>FB | A | 3 |

**TABLE 4.2: RESISTIVITIES OF SOME IGNEOUS, METAMORPHIC AND SEDIMENTARY ROCKS (Telford et al., 1976).**

| Rock type | Resistivity range (ohm-metre) |
|---|---|
| Granite | $3 \times 10^2 - 10^4$ |
| Granite porphyry | $4.5 \times 10^3$ (wet) – $10^4$ (dry) |
| Gneiss (various) | $6.8 \times 10^4$ (wet) – $3 \times 10^4$ (dry) |
| Sandstones | $1 – 6.4 \times 10^8$ |
| Argillites | $10 – 8 \times 10^2$ |
| Unconsolidated wet clay | 20 |
| Clays | 1 – 100 |
| Alluvium and Sands | 10 – 800 |

**TABLE 4.3: RESISTIVITY VALUES ADOPTED FOR THIS WORK**

| Rock type | Resistivity range (ohm-metre) |
|---|---|
| Fadama loam | 20 – 100 |
| Clay, Silt and Sand | 80 – 400 |
| Weathered Basement | 101 – 750 |
| Fresh Basement | 751 - ∞ |

### 4.2 Results and Deductions from the VES data.

For an analytical discussion of the results of the VES, the geologic equivalent of the geoelectric section for the points were drawn (figures 4.6 - 4.7), since the interpretation of the collected geoelectrical sounding data is meaningless without some reliable geological control or some data relating to the intrinsic resistivities of the various geoelectric areas (Worthington, 1977).

#### 4.2.1 Geoelectric Sections along profiles.

To obtain geoelectric section along a profile, the profile of interest is first drawn as shown in the map in Figure 3.1. The position of each VES point is marked out. The resistivity values beneath each VES point along with their depth positions are obtained using the interpretation data for the geoelectric cross sections automatically generated by a computer software (IPI2win). Appropriate resistivity boundaries in form of contour are then drawn through points of equal resistivity values following the resistivity ranges obtained for various rock types. The resulting map shows the depth and thickness of a rock material at a point. Such result is referred to as geologic section.

The geologic sections in this work, was drawn based on the following controls:

1. Typical resistivity values from previous works in the basement area provided acceptable values for various earth materials (Table 4.2 and 4.3). According to Hockney (1986), these values are reliable.
2. A hand dug well in the area also served as a control.
3. The lithology and aquifer borehole 2 log of Amina hostel, Ahmadu Bello University, Zaria also served as a control. The area is underlain by reddish brown topsoil having a

thickness of 6m, reddish brown sandy clay with 2m thickness, weathered basement with thickness of 17m extending to a depth of about 25m (Table 4.4)

**Table 4.4 Lithology and Aquifer Borehole 2 – Amina Hostel, Ahmadu Bello University. (Hydro Skill Limited)**

| Depth (m) | Thickness (m) | Lithology |
|---|---|---|
| 0 – 6 | 6 | Reddish-brown topsoil |
| 6 – 8 | 2 | Reddish-brown sandy clay |
| 8 – 25 | 17 | Weathered basement |
| 25 - Infinity | ∞ | Fresh crystalline rock |

### 4.2.2 PROFILE AB

The geologic section along this profile, suggests three (3) geologic layer cases along the profile (Figure 4.6(I)). The top layer whose resistivity ranges from 57 to 738Ωm and thickness from 1.19 to 3.90m with the thickest portion at VES CT6 (3.90m) is a sandy, clay and silt soil containing fadama loam (Table 4.3). The second layer whose resistivity values ranges from 107 to 326Ωm and thickness from 2.24 to 12.30m with the thickest portion at VES CT3 (12.30m) is an indicator of the weathered basement. Its freshness (fresh basement) increases downward forming a three layer lithology. The study area slopes towards the western azimuth along the Kubanni River. Hence, the highest thickness of the weathered rock around VES CT3 may be a result of this effect. The third layer which is the fresh basement rock cuts across the entire length of the profile, which is shallowest at VES

CT4 (5.13m) and deepest at VES CT3 (14.4m). The resistivity of this area ranges from 960 to 1931Ωm. The geologic section further shows an upward extension of fresh basement into the weathered basement at depth of 12.77m at VES CT5.

### 4.2.3 PROFILE CD

The geological section along this profile, suggests that the subsurface is made up of three (3) layers along the profile (Figure 4.6(II)). The top soil resistivity value ranges from 18 to 300Ωm and thickness ranging from 1.23m at VES CT9 to 1.36m at VES CT8 connected to another rock type. The second layer, appearing to be a weathered basement has resistivity ranging from 185 to 757Ωm and thickness ranging from 0.52 to 4.65m. The layer is very thin and extends toward the western region of the study area. The resistivity of the third layer ranges from 901 to 3162Ωm. The fresh basement is closer to the
surface around VES CT11 with resistivity value of 1000Ωm and its highest resistivity value appears at VES CT8 with a value of 3162Ωm.

### 4.2.4 PROFILE EF

The geologic section for this profile shows the presence of three (3) layers and two (2) layers at VES CT13 (Figure 4.6(III)). The top layer is thinnest at VES CT16 which is 1.21m thick and thickest at VES CT14 with a thickness of 2.42m. Its resistivity ranges from 9 to 135Ωm. The thickness of the second layer ranges from 2.48 to 9.49m and its resistivity is between 497 to 735Ωm. The range type here is generally weathered. The third layer is the fresh basement with the resistivity value ranging from 534 to 3574Ωm. It is shallowest at 2.48m to the bedrock at VES CT13 and deepest at 10.72m to the bedrock at VES CT17.

### 4.2.5 PROFILE GH

The geologic section for this profile shows three (3) layers extending all along its length (Figure 4.7(IV)). The topsoil has resistivity ranging from 20 to 320Ωm and thickness

ranging from 1.36 to 3.35m. The second layer of the geologic section also suggests that the thickest portion is at VES CT23 with a thickness of 10.10m and thinnest at VES CT21 with a thickness of 2.68m. The resistivity ranges between 97 and 442Ωm. The third (3) layer with resistivity value as low as 990Ωm and as high as 2257Ωm appears to be the fresh basement. The shallowest depth of the fresh basement was found to be about 4.64m at VES CT21 and deepest at depth 13.45m at VES CT23 along the chosen profile of the study area.

**4.2.6 PROFILE IJ**

The geologic section along this profile suggests three (3) layers extending all over the profile, (Figure 4.7(V)). The topsoil has resistivity ranging from 61 to 336Ωm and thickness ranging from 1.21m at VES CT34 to 3.91m at VES CT35. The geologic section also suggests that the second layer (weathered basement) is thickest at VES CT35 with a thickness of 23.00m and thinnest at VES CT34 with thickness of about 9.40m. The resistivity value ranges from 159 to 613Ωm. The third layer suggests to be a fresh basement has resistivity value as low 991Ωm and as high as 2859Ωm. The shallowest depth to the fresh basement (bedrock) was found to be 10.63m at VES CT34 and the deepest is 26.91m at VES CT35.

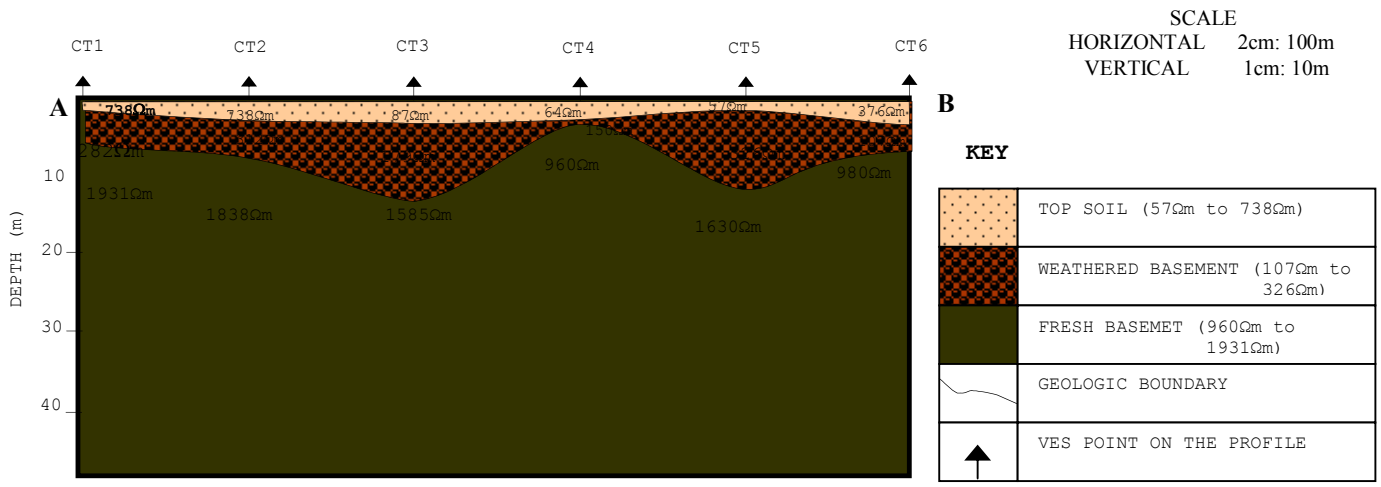
**4.2.7 PROFILE KL**

The geologic section along this profile suggests three (3) layers extending all over the profile, (Figure 4.7(VI)). The topsoil has resistivity ranging from 8 to 123Ωm and thickness ranging from 1.30m at VES CT29 to 1.94m at VES CT30. The geologic section also suggests that the second layer (weathered basement) is thickest around VES CT29 with a thickness of 19.50m and thinnest at VES CT27 with thickness of 0.60m. The resistivity value ranges from 229 to 987Ωm. The third layer suggests to be a fresh basement has resistivity value as low 990Ωm and as high as 6036Ωm. The shallowest depth to the fresh

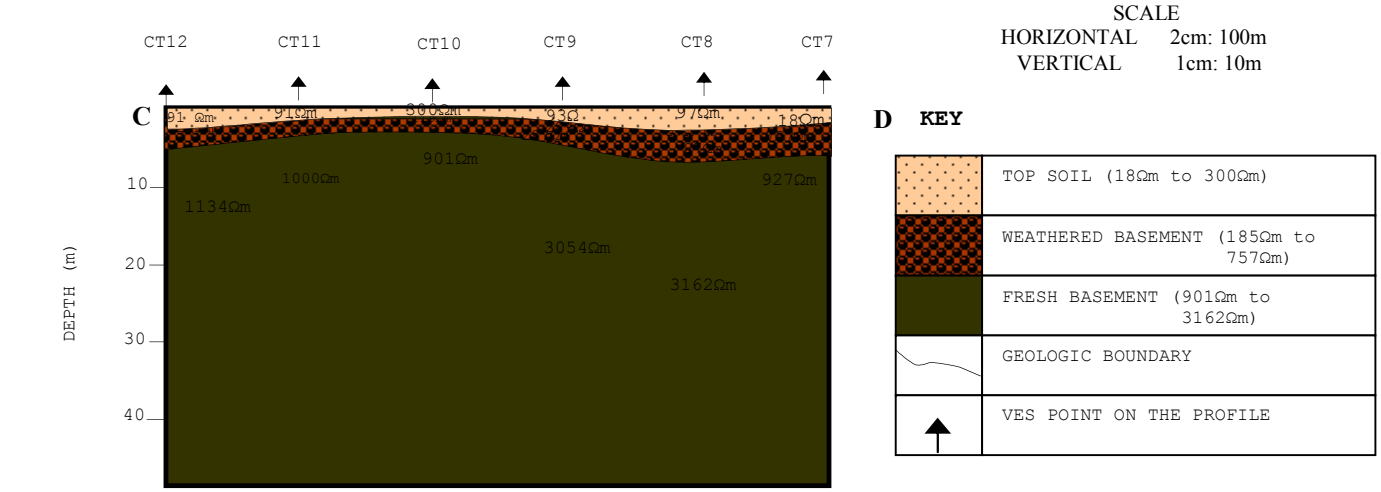
basement (bedrock) was found to be 2.29m at VES CT27 and deepest at VES CT29 with depth to bedrock to be 20.80m.

### 4.2.8 PROFILE MN

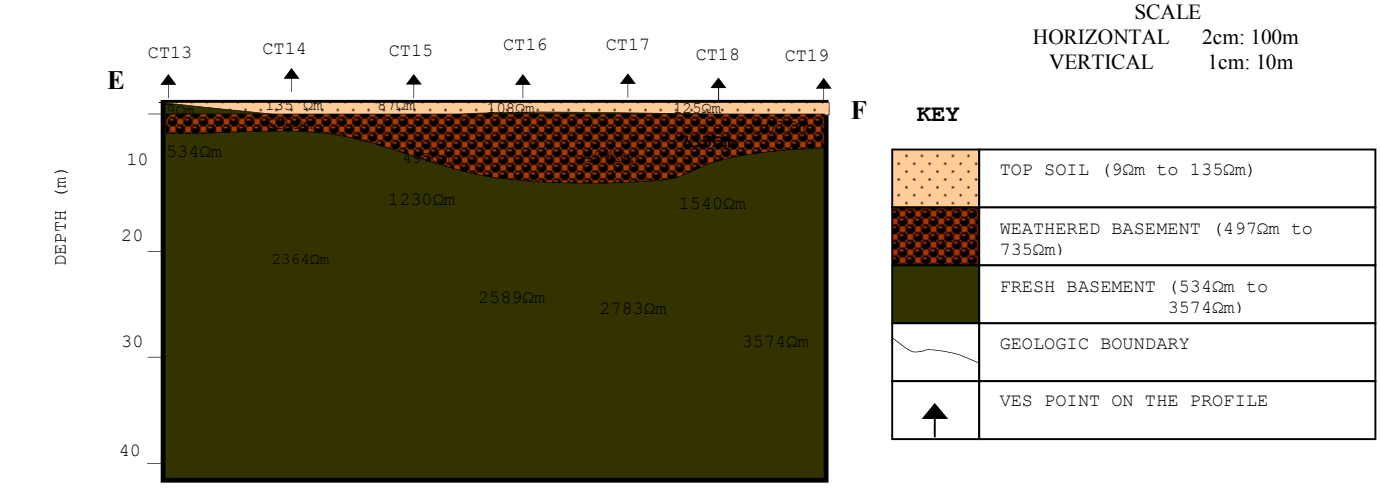
The geologic section along this profile suggests three (3) layers extending all over the profile, (Figure 4.7(VII)). The topsoil has resistivity ranging from 13 to 49Ωm and thickness ranging from 1.21m at VES CT39 to 2.24m at VES CT40. The geologic section also suggests that the second layer (weathered basement) is thickest at VES CT40 with a thickness of 10.80m and thinnest at VES CT38 with thickness of 3.43m. The resistivity value ranges from 159 to 681Ωm. The third layer suggests to be a fresh basement has resistivity value as low 521Ωm and as high as 3162Ωm. The shallowest depth to the fresh basement (bedrock) was found to be 5.15m at VES CT38 and the deepest depth is 12.84m at VES CT40.




I




II




III

**FIG. 4.6: GEOELECTRIC SECTIONS ALONG PROFILES AB, CD AND EF.**

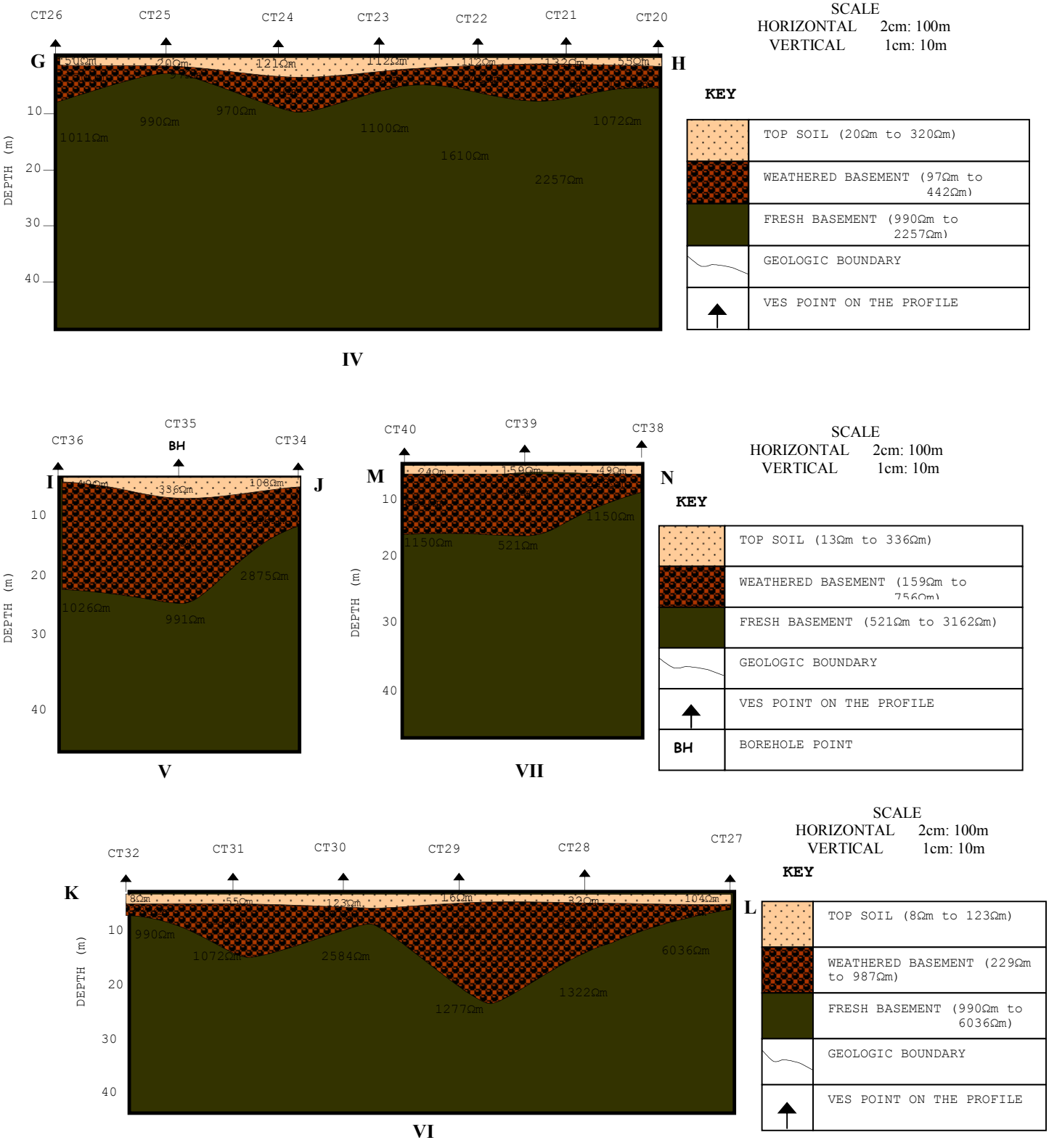



**FIG. 4.7: GEOELECTRIC SECTIONS ALONG PROFILES GH, MN, IJ AND KL.**

### 4.2.9 ISORESISTIVITY CONTOUR MAPS

The Isoresistivity contour maps have helped to show at a glance the resistivity distributions over the whole area at preferred depths. This work shows the isoresistivity map at 2.00m, 5.00m, 10.00m, 20.00m and 25.00m depth respectively. Equal resistivity values at various depths all over the study site were selected and contoured as shown in figure 4.8 to 4.12 below.

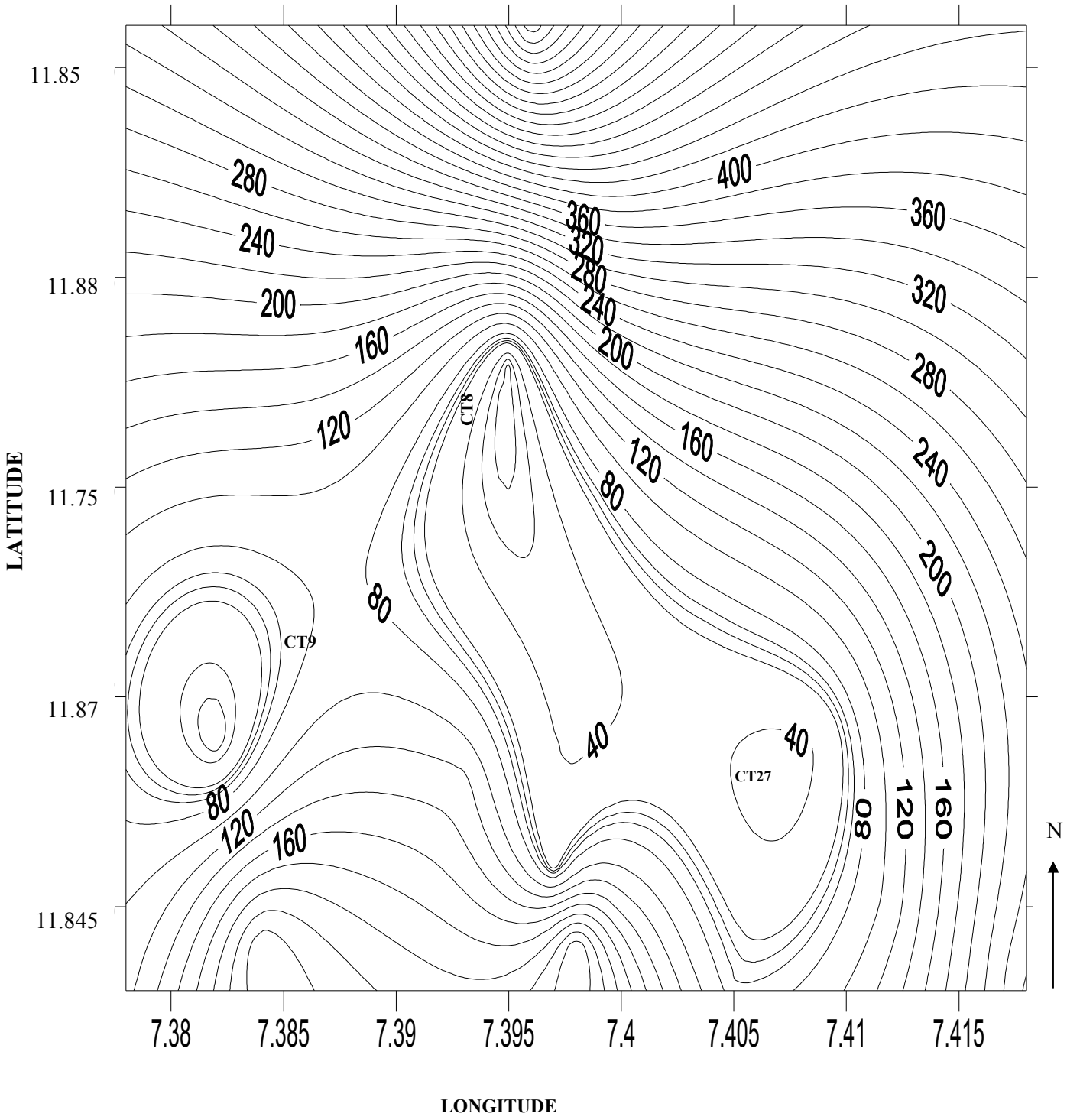



**FIG 4.8: Isoresistivity Map at 2.00m depth. Cont. Int. 20Ωm**

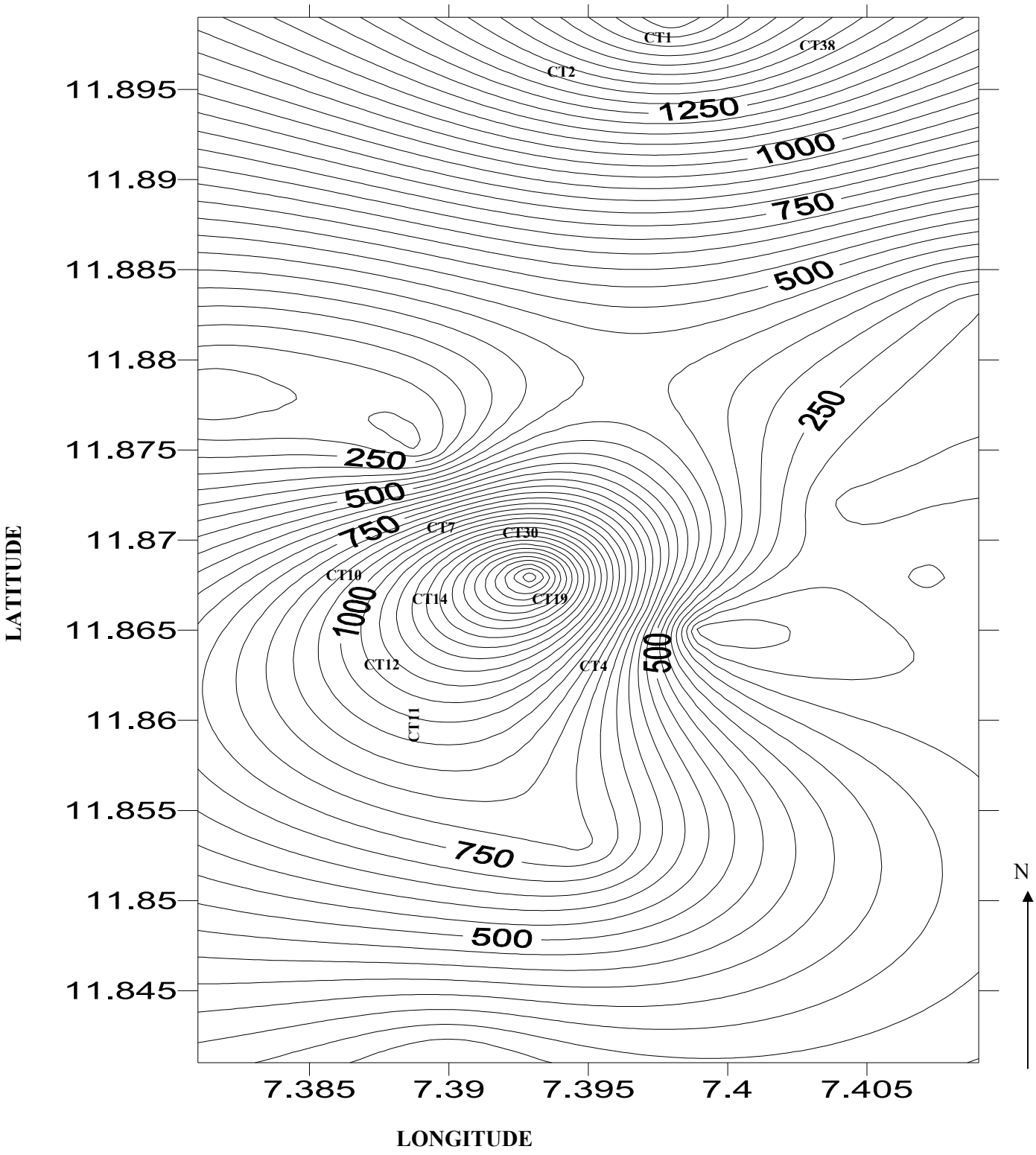



**FIG 4.9: Isoresistivity Map at 5.00m depth. Cont. Int. 50Ωm**

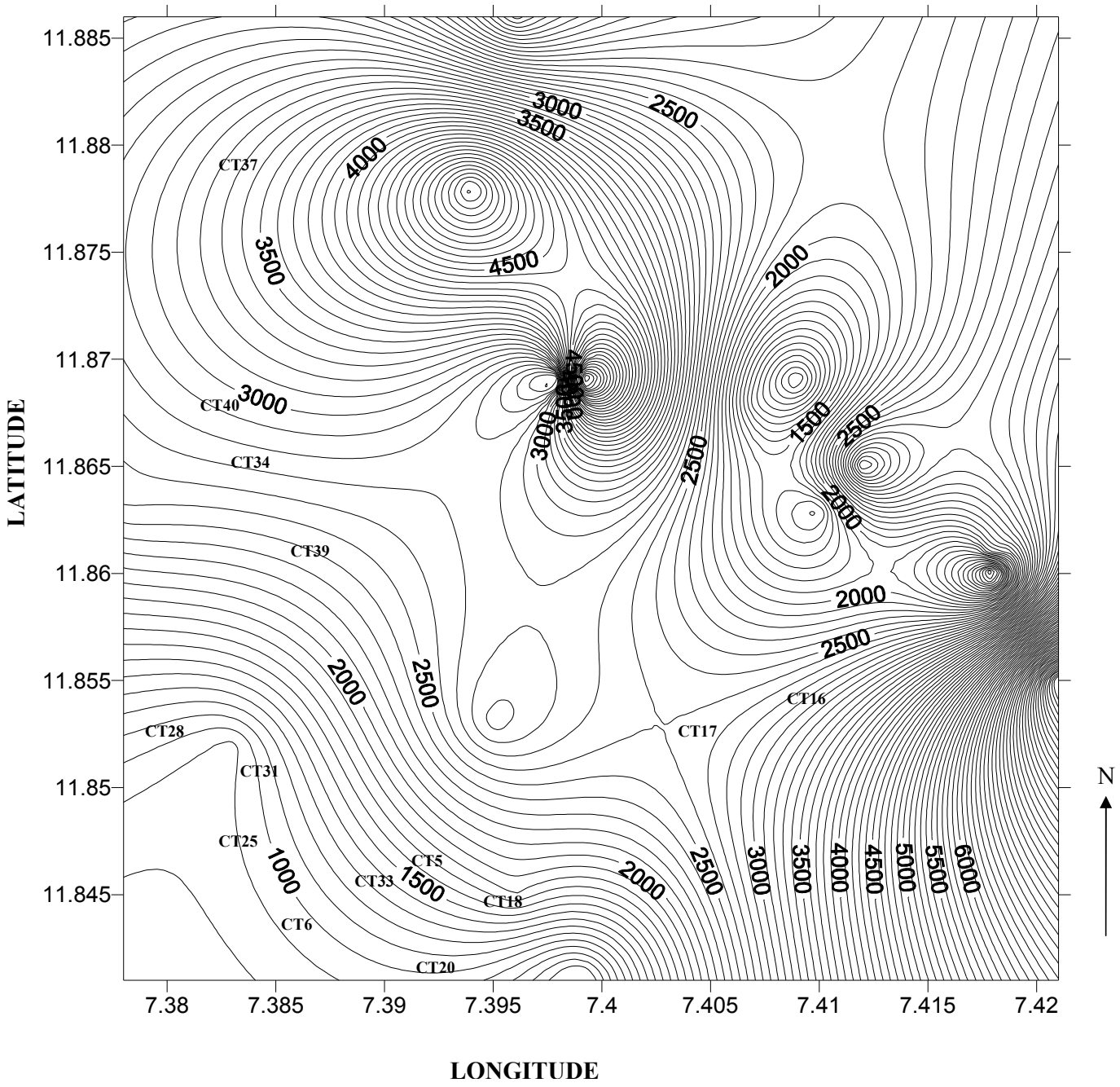



**FIG.4.10: Isoresistivity Map at 10.00m depth. Cont. Int. 100Ωm**

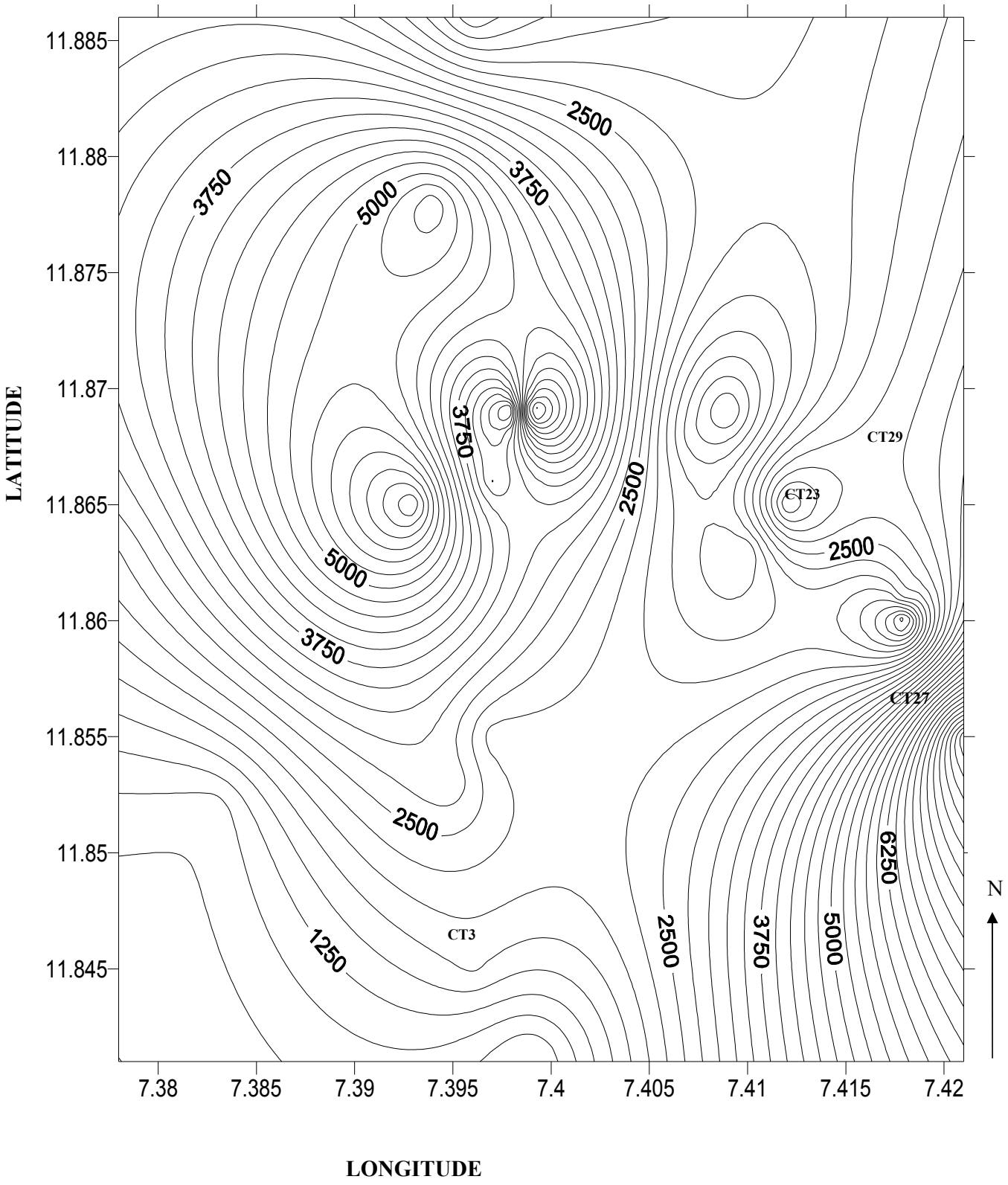



**FIG 4.11: Isoresistivity Map at 20.00m depth. Cont. Int. 250Ωm**

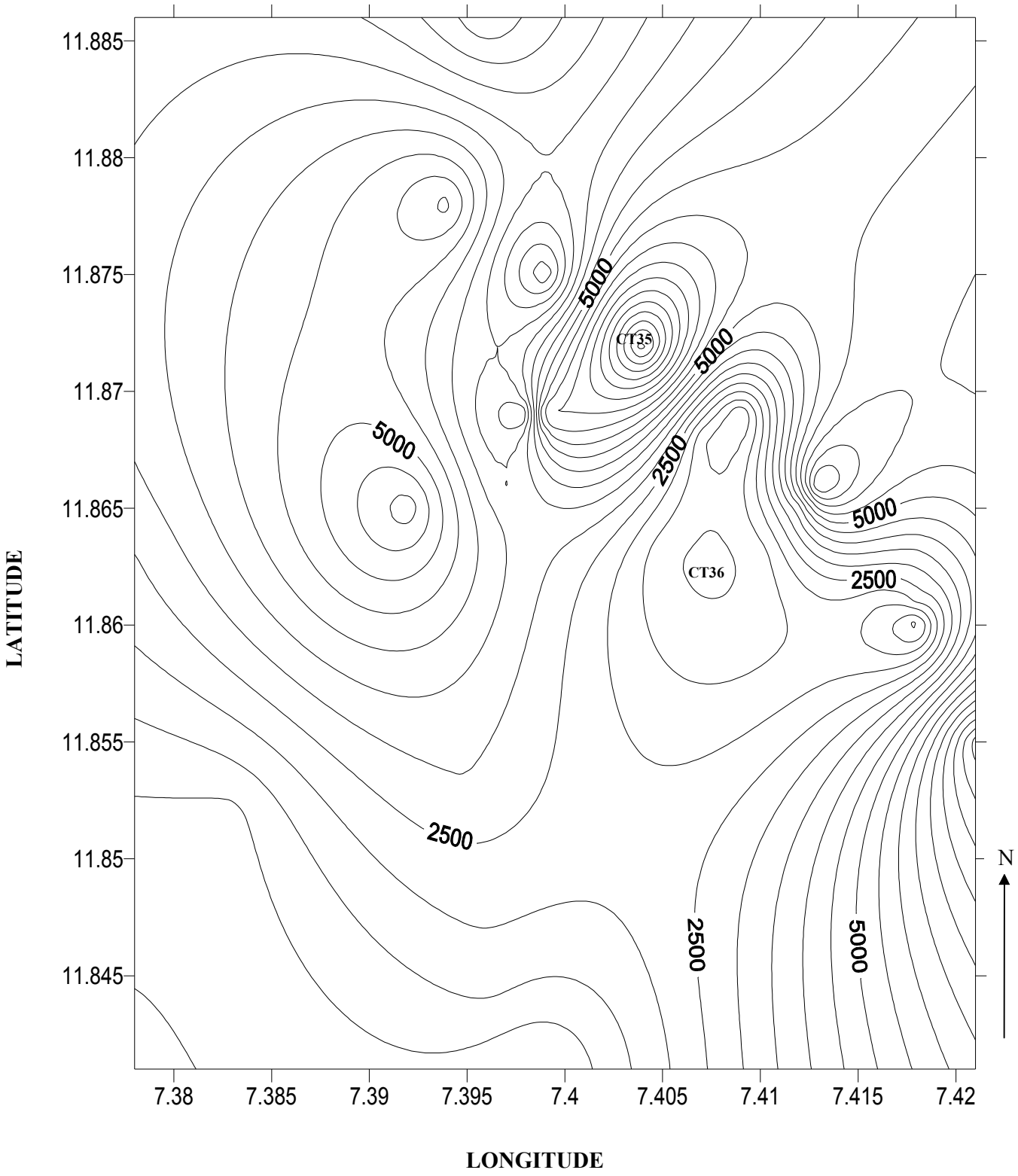


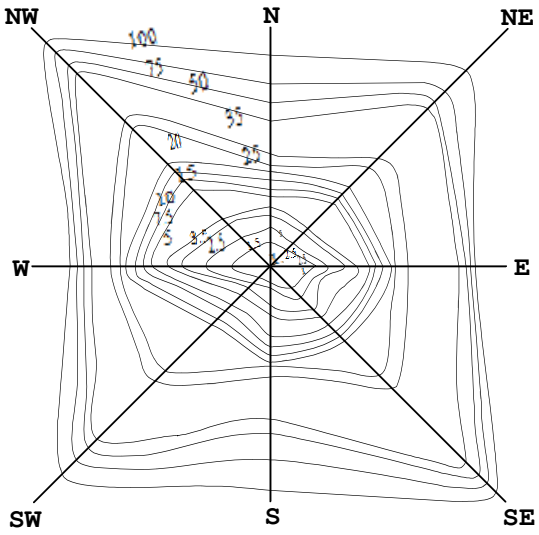

**FIG 4.12: Isoresistivity Map at 25.00m depth. Cont. Int. 500Ωm**

Figure 4.8 shows that the regions around VES CT8, CT9 and CT13 have the highest resistivity values at depth 2.00m while most of the other areas have low values due to the layer of silt and clay at the top layer (topsoil). However, the highly resistive area may indicate high content of sand and silt mixed with the topsoil at this depth.

Figure 4.9 shows a high resistivity value around VES CT10, CT11 and CT14 which is an indication of outcrop of fresh basement. This extends towards CT30 and CT38 while other areas have very low resistivity, which is an indication that the topsoil has been exceeded and another layer (weathered basement) that is a water bearing area i.e aquifer have been approached in some areas. These conditions persist down 20.00m and 25.00m respectively as shown in Figure 4.10, 4.11 and 4.12 while other areas of high resistivity are becoming prominent. Areas around CT33, CT34, CT35, CT36, CT37, CT38, CT39 and CT40 are examples of resistive spots. This situation continues as far as the last depth contour.

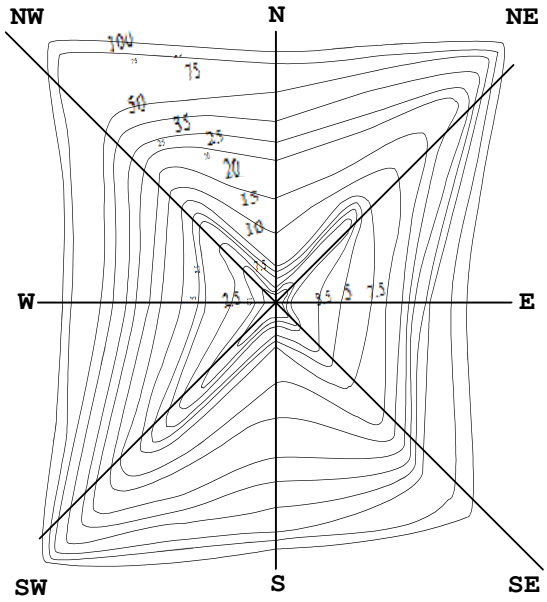
### 4.2.10 RESULTS FROM AZIMUTHAL SOUNDING PLOTS.

The azimuthal plots give an insight to the subsurface trend of resistivity anisotropy. The presence of resistivity anisotropy sometimes depict occurrence of fractures, faults, cracks or fissures which are the cognate structural elements (Telford et al., 1976, 1990). Their presence in a water bearing bed can serve as groundwater storage. In view of these, four (4) azimuthal soundings of four azimuths (i.e. N-S, E-W, NE-SW and NW-SE) were randomly established to cover the whole area. The azimuthal data were similarly reduced and a linear plot was obtained for apparent resistivity, ($\rho_a$), versus the electrode spacings ($1/2$AB) along each of the four azimuths.



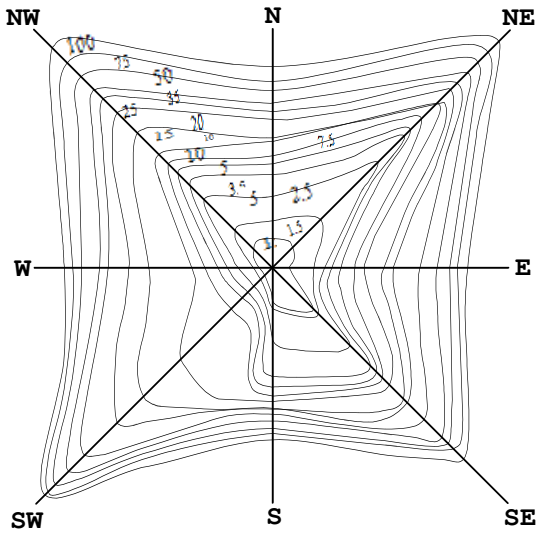

STATION CT18

**SCALE:** 1cm: 500Ωm



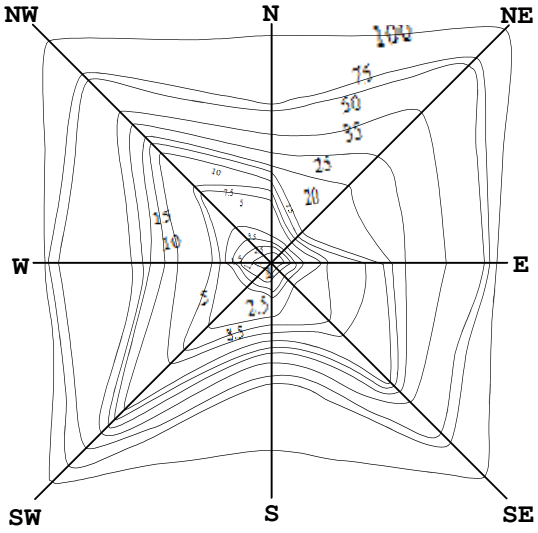

STATION CT 15

**SCALE:** 1cm: 500Ωm




STATION CT12

**SCALE:** 1cm: 500Ωm




STATION CT22

**SCALE:** 1cm: 500Ωm

**FIG. 4.13: PLOTS OF AZIMUTHAL SOUNDINGS AT STATIONS CT12, CT15, CT18 AND CT22**

Figure 4.13 shows the existence of resistivity anisotropy which varies with depth as indicated by the ellipses of the plots. Depths of anisotropic variation are classified as shallow, intermediate, and great depths. The directions and variation of the anisotropy obtained for the stations are summarized in the table below.

**Table 4.5: TRENDS OF SUBSURFACE RESISTIVITY ANISOTROPIES AS OBTAINED FROM THE AZIMUTHAL SOUNDING PLOTS.**

| Stations | Shallow depth | Intermediate depth | Great depth |
|---|---|---|---|
| CT12 | NIL | NW-SE | NE-SW |
| CT15 | NIL | NW-SE | NE-SW |
| CT18 | E-W | NE-SW | NW-SE |
| CT22 | E-W | NW-SE | NE-SW |

The above table shows a greater concentration of anisotropies at the intermediate and great depths. This on the other hand implies that the direction of resistivity anisotropies follow the major direction of faulting in the basement areas as shown by Oluyide and Udoh (1986). This conformed with the deformational trend of the two Orogenic events which have wide spread effect over the basement complex rocks. These Orogenic events are:

I. The Eburnearn Orogeny (1950 ± 250 M.a) and

II. The Pan-African Orogeny (600 ± 50 M.a)

During these orogenic events, large volumes of granite were emplaced and initial sedimentary rocks were thermally reactivated (Ajibade et al., 1988). Rocks of the Basement

Complex show a general NW-SE and NE-SW structural trend, which seem to lie parallel to the limbs of major folds.

**4.2.11 Depth-to- Bedrock map.**

The IPI2win software used for the interpretation of this work generates set of depths with the corresponding resistivity values for each layer. The depth estimates (sum of thicknesses from topsoil to fresh basement) gives the depth to the fresh basement (or bedrock depth) which is the last depth. These data are used to plot the depth-to-bedrock map (Figure 4.14) by picking all depth data corresponding to the resistivity assumed for bedrock at all VES points.

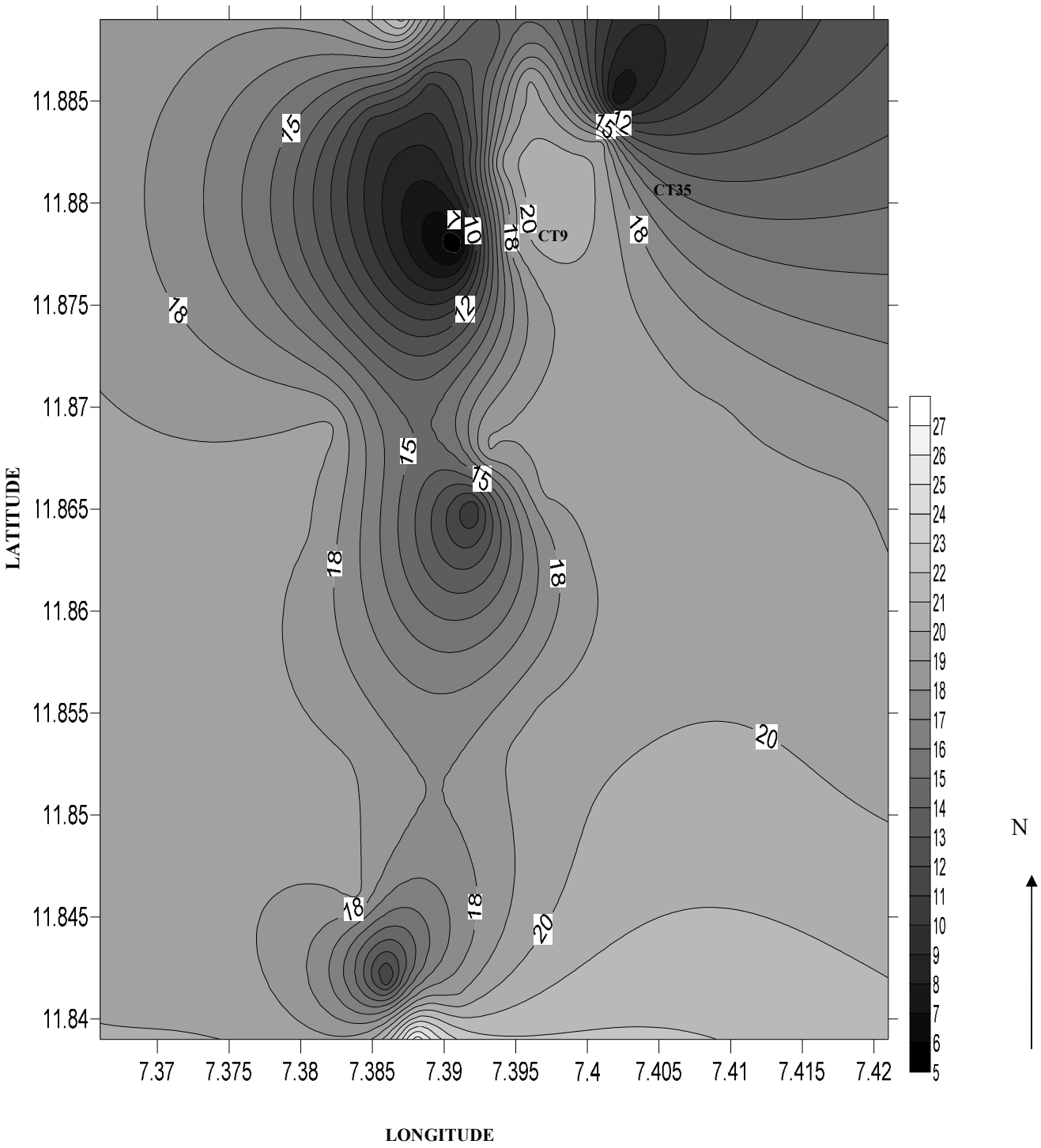



**FIG 4.14: Depth-to-Bedrock map. Cont. Int. 2.00m**

It can be seen that the bedrock is shallowest at VES CT9 with a depth of about 1.75m and deepest at VES CT35 with a depth of about 26.91m. A surface plot for the bedrock is shown in Figure 4.15 which is a representative of the bedrock topography.

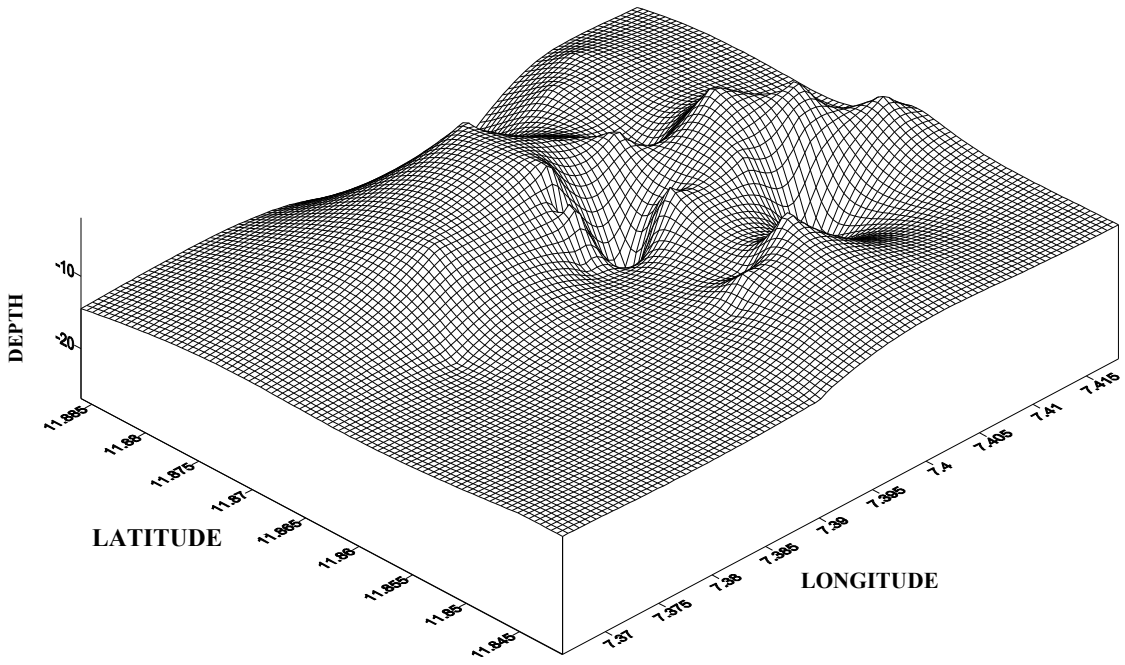



**FIG. 4.15: Surface Plot of the Bedrock.**

### 4.2.12 Depth-to-and thickness of Weathered Basement maps

In achieving depth and thickness of the weathered basement, data of depths, with the corresponding resistivity values of the assumed values for weathered basement were used. The same process is followed using the resistivity range values for the weathered basement to obtain its thickness distribution. Figures 4.16 and 4.17 were obtained with the two processes above. Figure 4.17 shows that weathered basement is deepest at VES CT35 with a depth of about 26.91m. The thickest portion as indicated by figure 4.16 of the weathered basement is about 23.00m which is around the same VES point i.e. CT35.

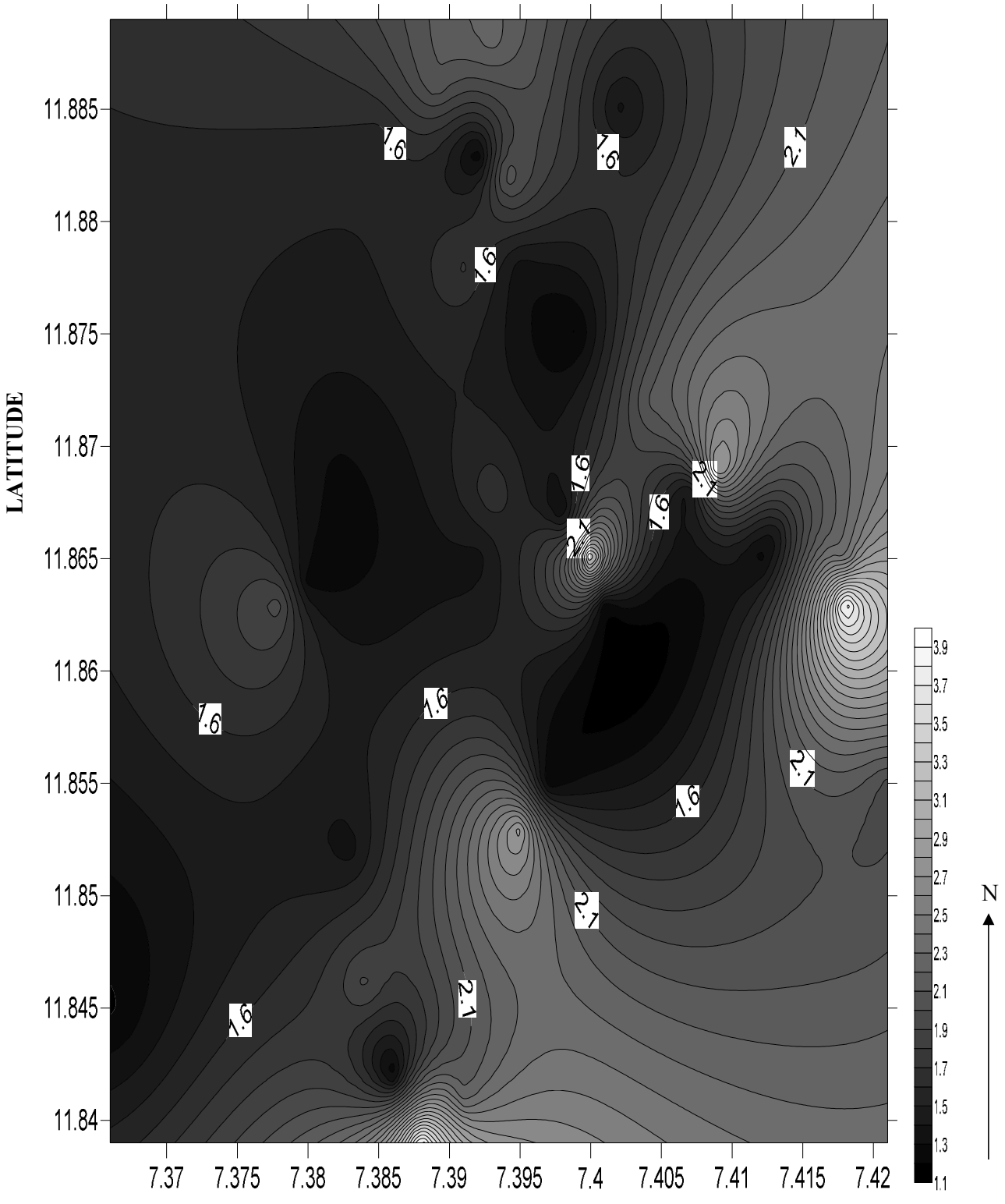



**FIG 4.16: Depth-to-Weathered Basement Map. Cont. Int. 0.20m**

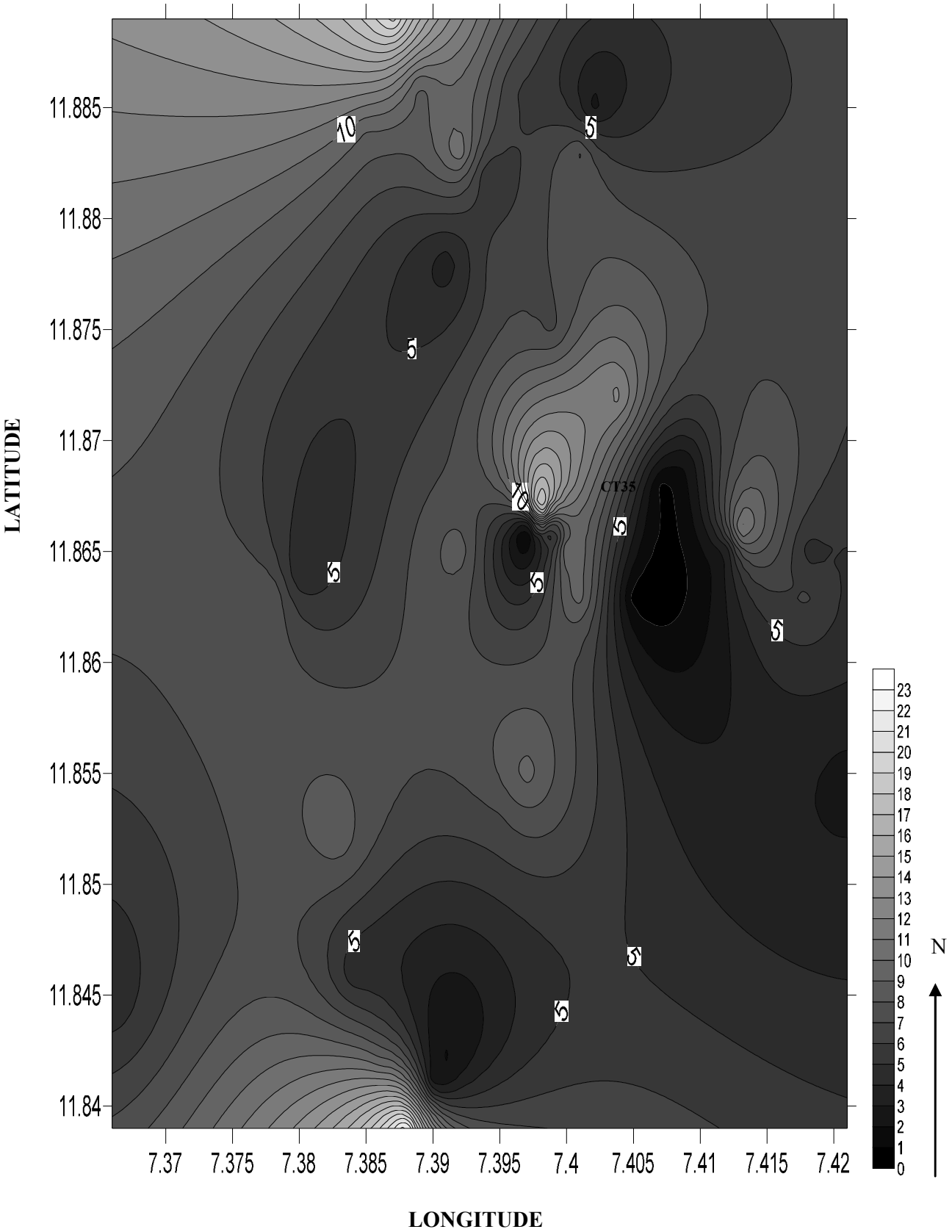



**FIG.4.17: Thickness-of-Weathered Basement map. Cont. Int.1.00m**

# CHAPTER FIVE

# DISCUSSION OF RESULTS, CONCLUSION AND RECOMMENDATION

## 5.1 GENERAL DISCUSSION OF RESULTS

The aim of this work was to investigate depth to the bedrock, determine thickness of the weathered basement, and structural (fracture) features in the area.

The VES carried out at forty (40) stations aided in deriving geologic sections equivalent to some geoelectric sections along some chosen profiles. These revealed that there are mostly three geologic layers (3 - layer cases) beneath each VES station, and a two layers geologic section at a point. The predominant layers are: the topsoil consisting of clay, silt and sandy soil. The resistivity of this layer is as low as 2Ωm and as high as 738Ωm on some profiles while the thickness range is from 1.00 to 3.90m. The weathered basement formed the second layer in most of the profiles with the resistivity value as low as 32Ωm and as high as 757Ωm on some profiles. The thickness ranges from 0.50 to 23.00m. The shallowest depth to bedrock is 1.75m and the deepest is 26.91m. The third layer is the fresh basement whose resistivity is as high as 6,036Ωm. The aquifer in the area is shallowest at 1.75m and deepest at 26.91m.

The azimuthal sounding results show some prevalent structural patterns and trends which are NE-SW, NW-SE and E-W. This is evident from the changing direction of resistivity anisotropies with depth, a phenomenon which is likely to be due to faulting. From the work of McCurry (1970), the structural pattern trending NE-SW is parallel to the Funtua transcurrent pattern. The changes in the direction of resistivity anisotropies with depth as revealed by the azimuthal sounding plots may be due to changes of tectonic activities and are classified as shallow, intermediate and great depth zones. A number of physical events are observed in the study area. The physical structures are located within VES point CT34, CT35

and CT36 respectively. The administration block is around VES (CT34). The depth to bedrock at this point is 10.63m, thickness of weathered basement is 9.42m and thickness of topsoil is 1.21m. These parameters are suitable for the structure as a result of the following reasons; It has a very thin topsoil (clayey). It has a shallow depth to bedrock. Bedrock often serve as pillar supports to buildings. Similarly, behind the reactor building is VES CT36, its depth to bedrock is 22.51m, thickness of weathered basement is 20.50m and thickness of topsoil is 2.01m. These parameters are suitable for the reactor site. It has a thick weathered basement (fracture zone). The borehole area is at VES CT35. The thickness of weathered basement is 23.00m, thickness of topsoil is 3.91m and depth to bedrock is 26.91m. The weathered basement is an aquifferous zone, highly fractured, having high degree of water saturation. The borehole bears water throughout the year which serves both domestic and industrial purposes in the study area because of its high thickness of weathered basement (fractured or aquiferrous zone) which could serve as a good water aquifer. Detailed information on the borehole was inadequate because the borehole log was not available which was a limitation to this work. This confirms that Centre for Energy Research and Training (CERT) is seated on a shallow basement.

A hand dug well located in CERT farm at VES CT11 has thickness of weathered basement of 4.06m, thickness of topsoil is 1.26m and its depth to bedrock is 5.32m. It is a shallow well but very close to the water table which in turn bears water throughout the year. The well is very important for their annual crop cultivation.

The guest house complex located at VES CT28 is said to be seated on a shallow aquifer, it has thickness of weathered basement of 7.32m, thickness of topsoil is 1.69m and its depth to bedrock is 9.01m. These parameters are suitable for the building.

## 5.2 CONCLUSION

In this work, the electrical d.c. resistivity method was employed to establish forty (40) VES points which offered complimentary solution to the problem of this investigation. The following conclusions are drawn from this work:

The study area is mostly characterized by three (3) layered geologic sections which include the topsoil, weathered basement and fresh basement. The topsoil has resistivity ranging from 2 to 738Ωm. The weathered basement has resistivity ranging from 32 to 757Ωm with depth ranging from 1.75 to 26.91m. The topsoil is fine grain rocks (clayey), associated with weathering of sulphide minerals from the underlying granitic rocks. They have great amount of dissolved salts resulting to low resistivity values. The weathered basement is deepest around VES CT35 with a depth of 26.91m. The thickest portion of the weathered basement is 23.00m at VES CT35. The weathered basements are medium to fine grain porous or fractured rocks containing water. They are referred to as the aquiferrous zone. Highly fractured areas have low resistivity because of its high degree of saturated water implying that their resistivity is greatly influenced by underground water. The fresh basement has its deepest part at VES CT35 of 26.91m located towards the western azimuth of the study area. The fresh basement rocks are coarse, close grained (plutonic or intrusive) rocks, constituting the rock forming minerals which are poor conductors.

The presence of some structural elements such as fractures or fissures were revealed by the existence of resistivity anisotropies in the subsurface rocks. These vary with depth and thus confirmed the occurrence of tectonic activities in the study area. The major resistivity anisotropy directions noticeable are NE-SW, NW-SE and E-W. These deformational trends

conform to the two major Orogenic events that have widespread effect over the country namely; the Eburnean and Pan-African Orogenies.

The study area is found to have shallow depth to the basement. Therefore, the following areas can be used for siting boreholes: VES CT3, CT5, CT23, CT29, CT36, CT39 and CT40. These points are chosen because they have considerable thickness of weathered basement (fractured zone > 10.00m) which could be a good water aquifer i.e. have identified elements for groundwater storage such as high porosity, permeability and less consolidation.

Strategic areas for siting high-rise buildings may include: VES CT30, CT28, CT26,

CT25, CT11, CT10, CT2, CT1, CT38 and CT37. These are areas with shallow depths to the bedrock (5.00 to 10.00m) and also thin topsoil (thickness < 5.00m) because of the clayey nature of the topsoil. The consolidated basement (bedrock) can serve as pillar supports for buildings. Since study area has shallow depths to the bedrock and water aquifer, the depth of sewage system should be < 10.00m to the aquiferrous zone (weathered basement) in order to avoid groundwater contamination.

**5.4 RECOMMENDATION**

The investigation was accomplished using one of the geophysical methods which is the electrical resistivity method. Other geophysical methods such as, seismic (refraction), magnetics, gravity and VLF methods which are found to be greatly instrumental in mapping subsurface materials and determining depth to bedrock, can be used to continue the findings from this study.

## REFERENCES


Ajibade, A.C., Rahaman, M.A. and Ogezi, A.E.O., (1988): *The Precambrian Geochronology of Precambrian Geology of Nigeria, Review in Geology of Nigeria* (ed. C.A. Kogbe), Elizabethan Publ. Co., Lagos, P. 312 – 314.

Ajibade, A.C., Woakes, M. and Rahaman, M.A., (1989): *Proterozoic Crustal Development in the Pan African Regime of Nigeria, Review in Geology of Nigeria* (ed. C.A. Kogbe), Elizabethan Publ. Co., Lagos, P. 70 - 80.

Akpoborie, I.A. (1973): *Hydrological Control of Structures along Samaru Creek.* Unpublished B.Sc. Thesis, Department of Geology, Ahmadu Bello University,Zaria.

Archie, G.E., (1942): *The electrical resistivity log as an aid in determining some reservoir characteristics*. Trans. A.I.M.E. 146, P. 54 – 62.

Barker, R.D., (1989): *Depth of Investigation of Collinear Symmetrical four-electrode arrays.* Geophysics, Vol. 54, No.6, P. 1031 – 1037.

Danladi, G.G., (1985): *Appraisal of Hydrological Investigation in Shallow Basement Area of Zaria*. Unplished M.Sc. Thesis, Department of Physics, Ahmadu Bello University, Zaria.

Dobrin, M. B. and Savit, C. H., (1988): *Introduction to Geophysical Prospecting*. *Fourth Edition*. McGraw-Hill Book Co.

Eigbefo, C., (1978): *Hydrology of Kubanni Drainage Basin, Zaria*. Unpublished M.Sc. Thesis, Department of Geology, Ahmadu Bello University, Zaria.

Farouq, A.U., (2001): *Geoelectric Investigation of the groundwater potential in the Institute for Agricultural Research farm*. Unpublished M.Sc. Thesis, Department of Physics, Ahmadu Bello University, Zaria.

Harold, E.D., (1970): *Arid Lands in Transition*. The Hornshafer Company Division of G.D.W. King Printing Co., U.S.A.

Hassan, M., (1987): *Geoelectrical Investigation of the Western Half of the Kubanni Basin, Zaria.* Unpublished M.Sc. Thesis, Department of Physics, Ahmadu Bello University, Zaria.

Hockney, R.D., (1986): *The Geology of the Lokoja – Auchi Area, Sheet 62.* G.S.N. Bulletin, No. 39, P 72 – 81.

Hore, P.N., (1970): *Weather and Climate: Review in Zaria and its Region* (ed. M. J. Mortimore), Department of Geography, Occasional Paper, No. 4, Ahmadu Bello University, Zaria, P. 41 – 54.

Kearey, P. and Brooks, M., (1984): *An Introduction to Geophysical Exploration, Geoscience*, Text, Published by Blackwell Scientific Publications.

Klinkenbera, K., (1970): *Soil of Zaria Area*. *Review in Zaria and its Region (*ed. M. J. Mortimore), Department of Geography, Occasional Paper, No. 4, Ahmadu Bello University, Zaria, P. 80 – 91.

Kunetz, G., (1966): *Principles of D.C. Resistivity Prospecting. Geoexploration Monographs*, Series No. 1, Gebruder Borntraeger, Berlin.

McCurry, P., (1970): *The Geology of Zaria Sheet 102*. Unpublished M.Sc. Thesis, Department of Geology, Ahmadu Bello University, Zaria.

McCurry, P., (1976): *The Geology of the Precambrian to lower Paleozoic rocks of Northern Nigeria, Review in Geology of Nigeria* (ed. C.A. Kogbe), Elizabethan Publ. Co., Lagos, P 15 – 40.

Obaje, N.G., Nzegbuna, A.I., Moumouni,A., Chaanda, M.S. and Goki, N.G., (2006): *Geology and Mineral Resources of Nasarawa State*. An investor's Guide, Nasara Scientifique, 2, P 34.

Olowu, J., (1967): *Preliminary Investigations of the Groundwater conditions in Zaria, Sheet 102 SW*. G.S.N.Report No. 1462.

Olufemi, R.O., (1985): *Hydrology of Jama'a Kubanni Area, Zaria Sheet 102 SW*. Unpublished B.Sc. Thesis, Department of Geology, Ahmadu Bello University, Zaria.

Oluyide, P.O. and Udoh, A., (1986): *Major Fracture System of Nigeria*, *In Precambrian Geology of Nigeria*, Geological Survey of Nigeria Pub., P 111 – 114.

Oyawoye, M.O., (1964): *Geology of Nigerian Basement Complex*. Journal of Mining and Geology. Vol. 1, P 110 -121.

Oyawoye, M.O., (1972): *The Basement Complex of Nigeria. Review in Africa Geology* (eds. Dessauvage and Whiteman), Geology Department, University of Ibadan, Nigeria, P 67 – 70.

Rahaman, M.A., (1972): *The late Precambrian to early Paleozoic Pan African Oregeny.* Nigeria. Geological Society of America, Bulletin, 80, P 78 – 85.

Rahaman, M.A., (1975): *Recent Advances in the Study of the Basement Complex of Nigeria, In Precambrian Geology of Nigeria*, Geological Survey of Nigeria Pub., P 11 – 44.

Parasnis, D.S., (1962): *Principles of Applied Geophysics*, Chapman and Hall Ltd., London.

Saminu, O., (1999): *Geophysical Investigation of Federal College of Education, Zaria.* Unpublished M.Sc. Thesis, Department of Physics, Ahmadu Bello

University, Zaria.

Telford,W.M, Geldart, L.P, Sheriff, R.E and Keys, D.A., (1976): *Applied Geophysics*. Cambridge University Press, London.

Telford,W.M, Geldart, L.P and Sheriff, R.E., (1990): *Applied Geophysics*, *Second Edition.* Cambridge University Press, London.

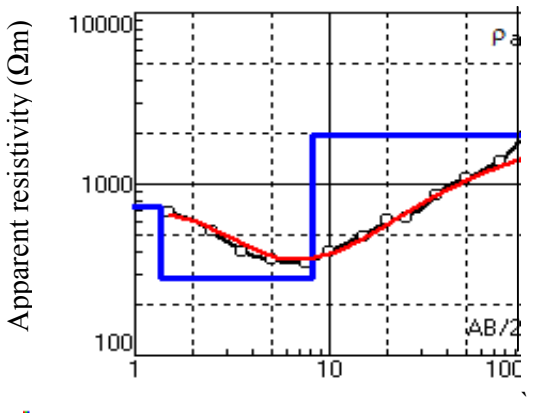
Thorp, M.B., (1970): *Land forms and Land Scape Evolution, Review in Zaria and its Region* (ed. M. J. Mortimore), Department of Geography, Occasional Paper, No. 4, Ahmadu Bello University, Zaria, P 141 – 150.

Webb, P.K., (1972): *Notes on Recent Research on the Geology between Zaria and Kaduna*, Savannah, Vol. 1, No. 2, P 41 – 52.

Worthington, P.F., (1977): *Geophysical Investigation of Groundwater Resources in the Kalahari Basin*, Geophysics, Vol. 42, P 838 – 849.

**APPENDIX**

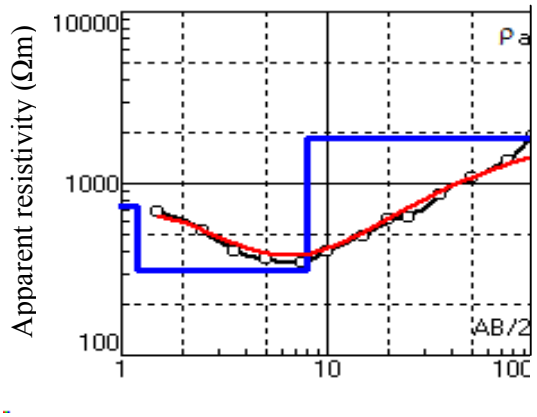
**VES RESULTS FOR THE ACQUIRED FIELD DATA.**




Electrode spacing (m)

CURVE AT VES CT 1 (TYPE H)

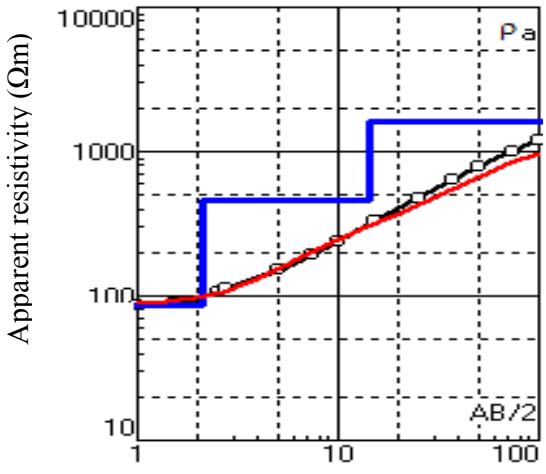
| N | ρ | h | d |
|---|---|---|---|
| 1 | 738 | 1.35 | 1.35 |
| 2 | 282 | 6.81 | 8.16 |
| 3 | 1931 | | |
| | | | |




Electrode spacing (m)

CURVE AT VES CT 2 (TYPE H)

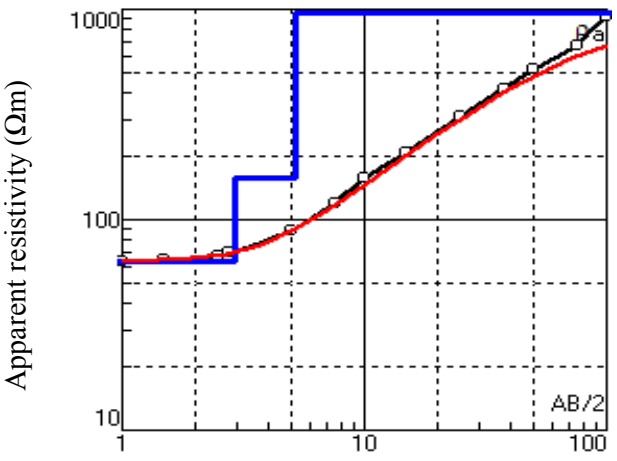
| N | ρ | h | d |
|---|---|---|---|
| 1 | 738 | 1.19 | 1.19 |
| 2 | 312 | 6.77 | 7.96 |
| 3 | 1835 | | |
| | | | |




Electrode spacing (m)

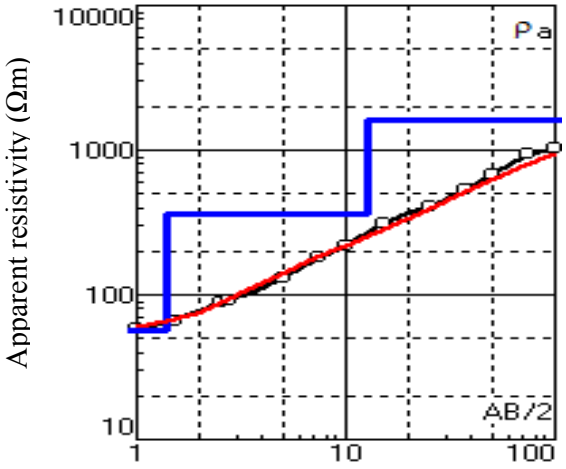
CURVE AT VES CT 3 (TYPE A)

| N | ρ | h | d |
|---|---|---|---|
| 1 | 87 | 2.11 | 2.11 |
| 2 | 460 | 12.3 | 14.4 |
| 3 | 1585 | | |
| | | | |



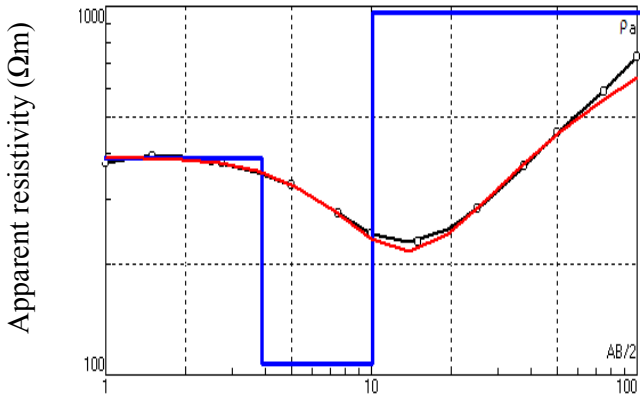

| N | ρ | h | d |
|---|---|---|---|
| 1 | 63 | 2.89 | 2.89 |
| 2 | 150 | 2.24 | 5.13 |
| 3 | 960 | | |
| | | | |

Electrode spacing (m)
CURVE AT VES CT 4 (TYPE A)



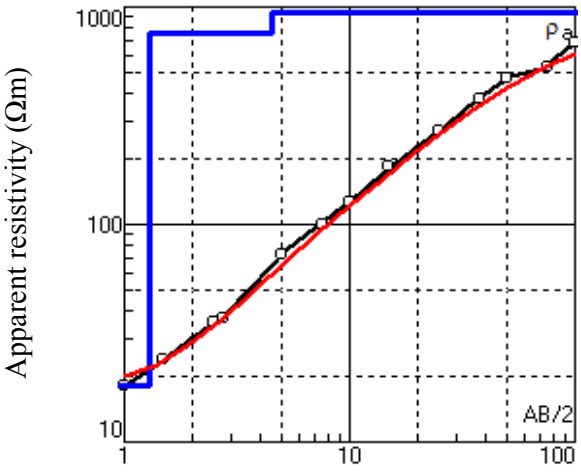

| N | ρ | h | d |
|---|---|---|---|
| 1 | 57 | 1.37 | 1.37 |
| 2 | 326 | 11.4 | 12.77 |
| 3 | 1630 | | |
| | | | |

Electrode spacing (m)
CURVE AT VES CT 5 (TYPE A)



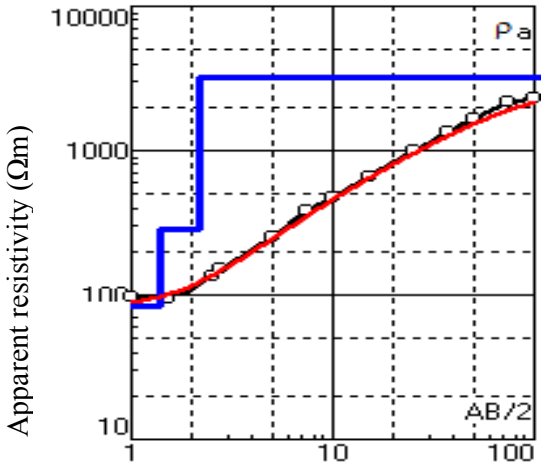

| N | ρ | h | d |
|---|---|---|---|
| 1 | 376 | 3.9 | 3.9 |
| 2 | 105 | 6.2 | 10.1 |
| 3 | 980 | | |
| | | | |

Electrode spacing (m)
CURVE AT VES CT 6 (TYPE H)



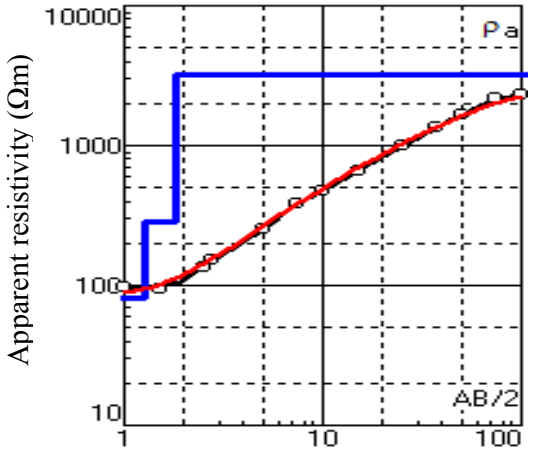

CURVE AT VES CT 7 (TYPE A)

| N | ρ | h | d |
|---|---|---|---|
| 1 | 18 | 1.26 | 1.26 |
| 2 | 757 | 3.2 | 4.46 |
| 3 | 927 | | |



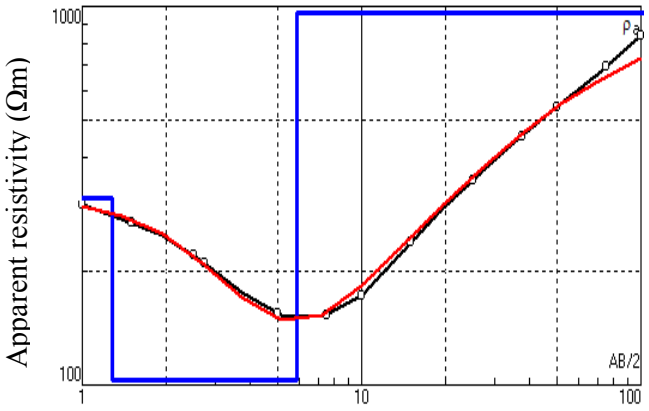

CURVE AT VES CT 8 (TYPE A)

| N | ρ | h | d |
|---|---|---|---|
| 1 | 97 | 1.36 | 1.36 |
| 2 | 287 | 0.78 | 2.15 |
| 3 | 3162 | | |
| | | | |



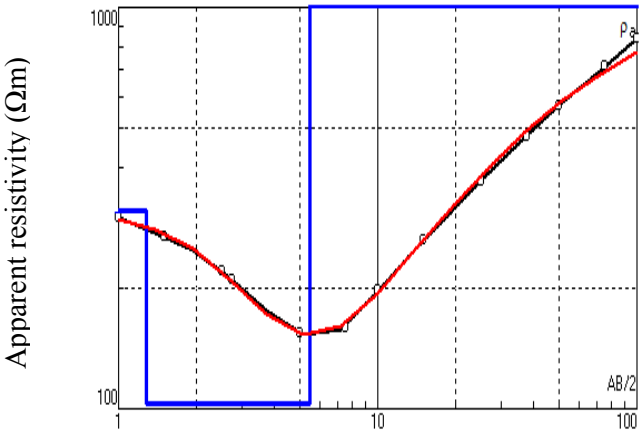

CURVE AT VES CT 9 (TYPE A)

| N | ρ | h | d |
|---|---|---|---|
| 1 | 93 | 1.23 | 1.23 |
| 2 | 287 | 0.52 | 1.75 |
| 3 | 3054 | | |
| | | | |



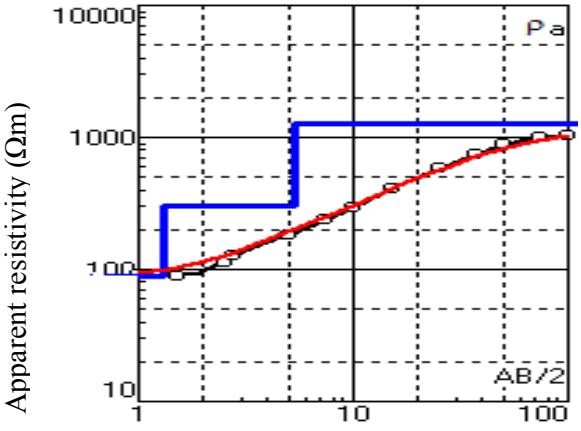

CURVE AT VES CT 10 (TYPE H)

| N | ρ | h | d |
|---|---|---|---|
| 1 | 300 | 1.28 | 1.28 |
| 2 | 119 | 4.65 | 5.93 |
| 3 | 990 | | |
| | | | |



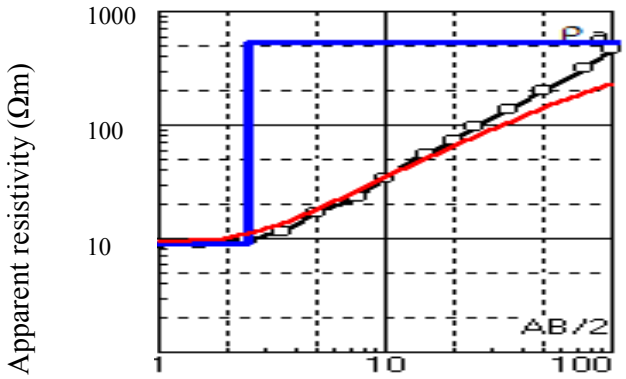

CURVE AT VES CT 11 (TYPE H)

| N | ρ | h | d |
|---|---|---|---|
| 1 | 296 | 1.26 | 1.26 |
| 2 | 185 | 4.06 | 5.32 |
| 3 | 1000 | | |
| | | | |



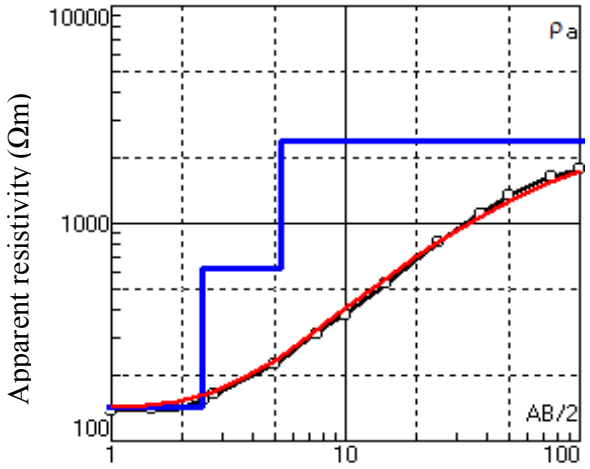

CURVE AT VES CT 12 (TYPE A)

| N | ρ | h | d |
|---|---|---|---|
| 1 | 91 | 1.18 | 1.18 |
| 2 | 321 | 4.08 | 5.26 |
| 3 | 1134 | | |
| | | | |



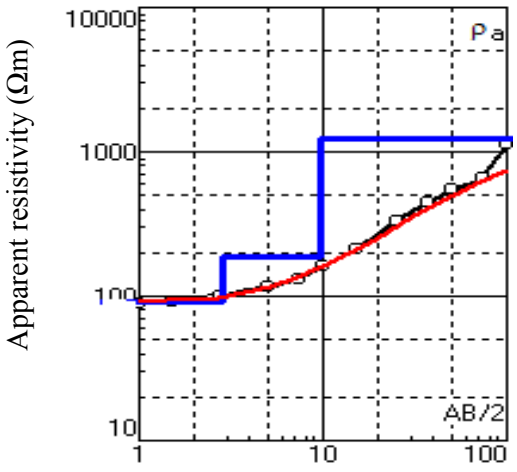

CURVE AT VES CT 13 (Two layers)

| N | ρ | h | d |
|---|---|---|---|
| 1 | 9 | 2.48 | 2.48 |
| 2 | 534 | | |
| | | | |



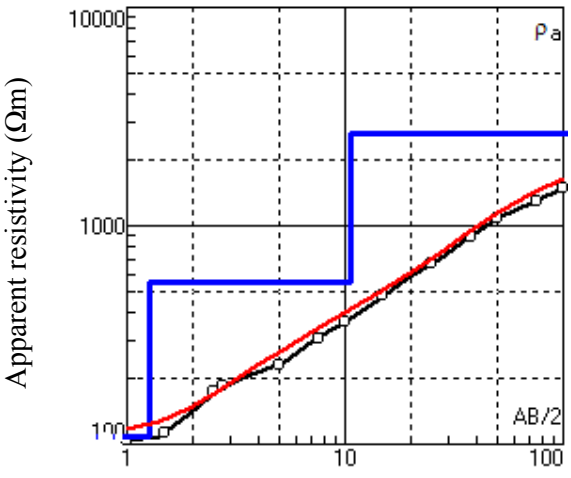

CURVE AT VES CT 14 (TYPE A)

| N | ρ | h | d |
|---|---|---|---|
| 1 | 135 | 2.42 | 2.42 |
| 2 | 618 | 2.76 | 5.18 |
| 3 | 2364 | | |
| | | | |



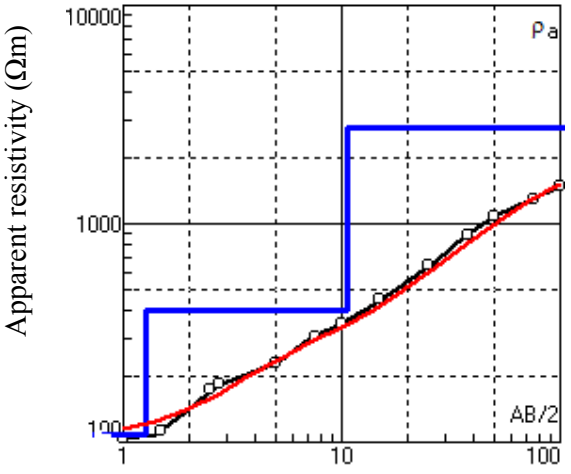

CURVE AT VES CT 15 (TYPE A)

| N | ρ | h | d |
|---|---|---|---|
| 1 | 89 | 2.85 | 2.85 |
| 2 | 197 | 6.86 | 9.71 |
| 3 | 1230 | | |
| | | | |



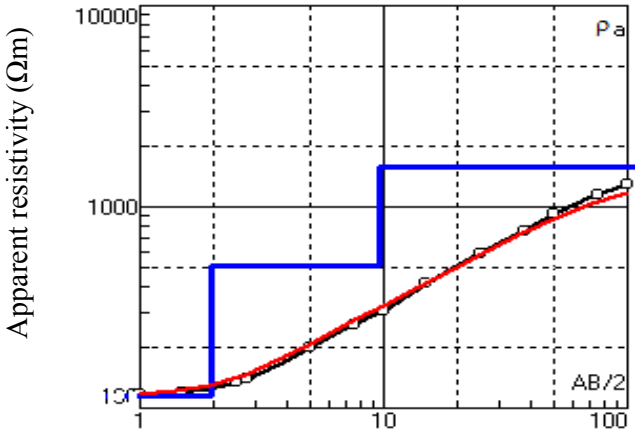

CURVE AT VES CT 16 (TYPE A)

| N | ρ | h | d |
|---|---|---|---|
| 1 | 108 | 1.21 | 1.21 |
| 2 | 546 | 9.42 | 10.63 |
| 3 | 2859 | | |
| | | | |



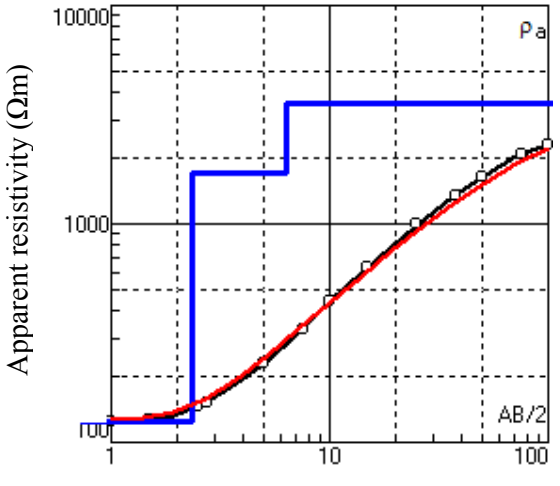

CURVE AT VES CT 17 (TYPE A)

| N | ρ | h | d |
|---|---|---|---|
| 1 | 107 | 1.23 | 1.23 |
| 2 | 404 | 9.49 | 10.7 |
| 3 | 2783 | | |
| | | | |



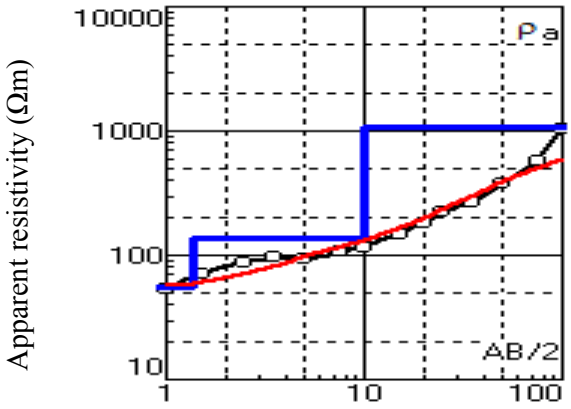

CURVE AT VES CT 18 (TYPE A)

| N | ρ | h | d |
|---|---|---|---|
| 1 | 118 | 1.95 | 1.95 |
| 2 | 501 | 7.94 | 9.89 |
| 3 | 1540 | | |
| | | | |



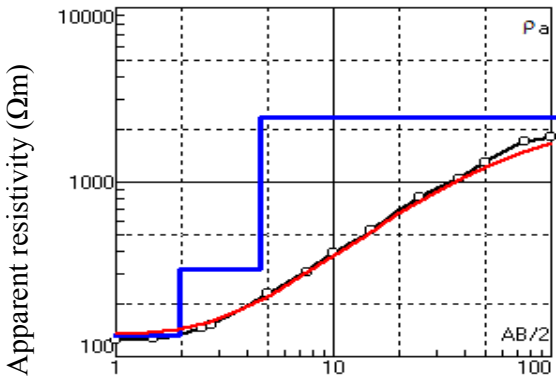

CURVE AT VES CT 19 (TYPE A)

| N | ρ | h | d |
|---|---|---|---|
| 1 | 125 | 1.94 | 1.94 |
| 2 | 1735 | 4.34 | 6.28 |
| 3 | 3574 | | |
| | | | |



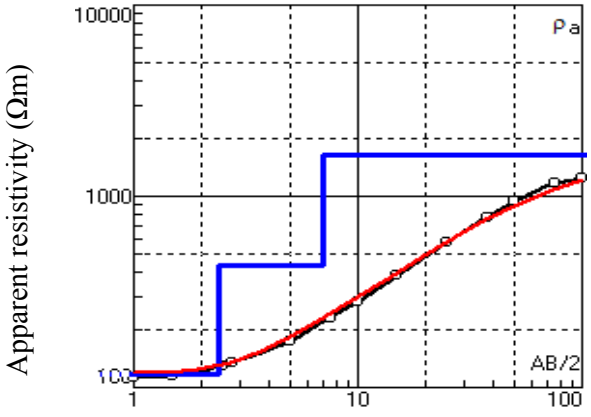

CURVE AT VES CT 20 (TYPE A)

| N | ρ | h | d |
|---|---|---|---|
| 1 | 55 | 1.36 | 1.36 |
| 2 | 116 | 8.65 | 10.01 |
| 3 | 1072 | | |
| | | | |



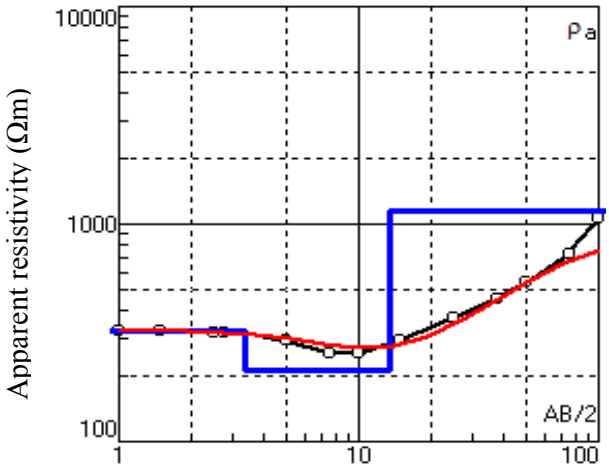

CURVE AT VES CT 21 (TYPE A)

| N | ρ | h | d |
|---|---|---|---|
| 1 | 132 | 1.96 | 1.96 |
| 2 | 313 | 2.68 | 4.64 |
| 3 | 2257 | | |
| | | | |



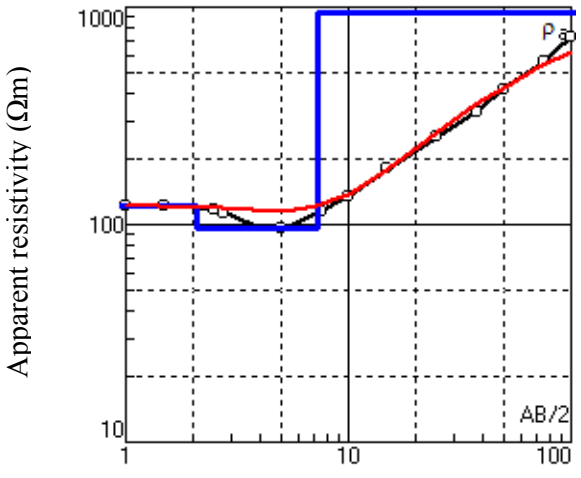

CURVE AT VES CT 22 (TYPE A)

| N | ρ | h | d |
|---|---|---|---|
| 1 | 112 | 2.4 | 2.4 |
| 2 | 442 | 4.61 | 7.01 |
| 3 | 1610 | | |
| | | | |



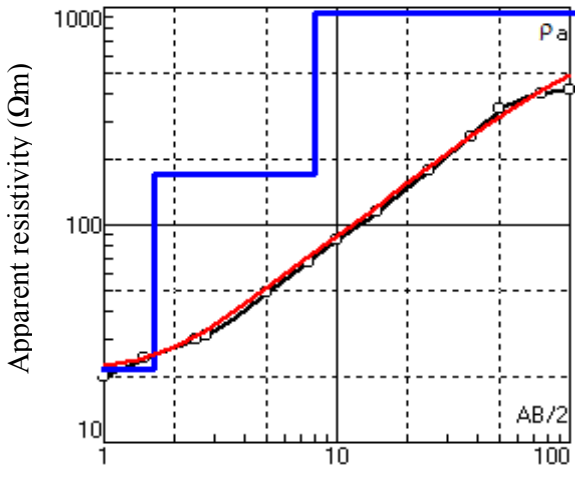

CURVE AT VES CT 23 (TYPE H)

| N | ρ | h | d |
|---|---|---|---|
| 1 | 320 | 3.35 | 3.35 |
| 2 | 236 | 10.1 | 13.5 |
| 3 | 1110 | | |
| | | | |




CURVE AT VES CT 24 (TYPE H)

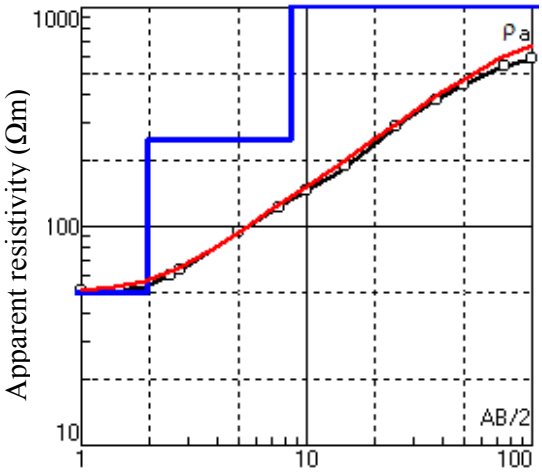
| N | ρ | h | d |
|---|---|---|---|
| 1 | 121 | 2.08 | 2.08 |
| 2 | 97 | 5.23 | 7.31 |
| 3 | 944 | | |
| | | | |




Electrode spacing (m)

CURVE AT VES CT 25 (TYPE A)

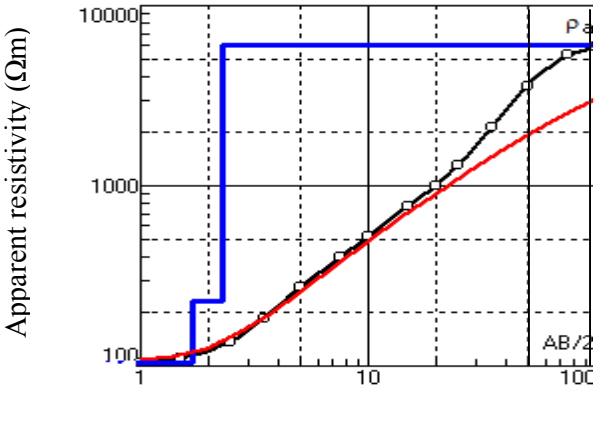
| N | ρ | h | d |
|---|---|---|---|
| 1 | 20 | 1.63 | 1.63 |
| 2 | 170 | 8.08 | 9.71 |
| 3 | 990 | | |
| | | | |




Electrode spacing (m)

CURVE AT VES CT 26 (TYPE A)

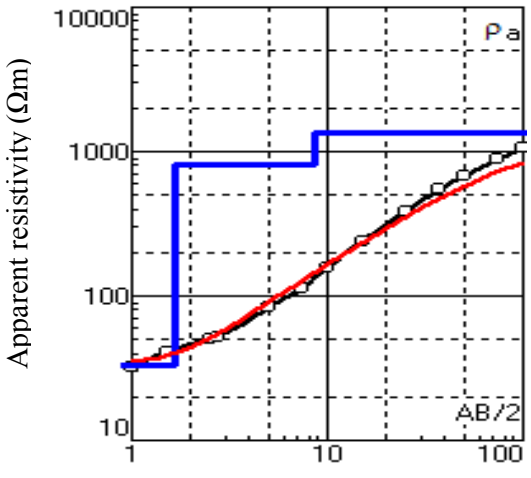
| N | ρ | h | d |
|---|---|---|---|
| 1 | 50 | 1.99 | 1.99 |
| 2 | 249 | 6.12 | 8.11 |
| 3 | 1011 | | |
| | | | |




Electrode spacing (m)

CURVE AT VES CT 27 (TYPE A)

| N | ρ | h | d |
|---|---|---|---|
| 1 | 104 | 1.69 | 1.69 |
| 2 | 229 | 0.6 | 2.29 |
| 3 | 6036 | | |
| | | | |

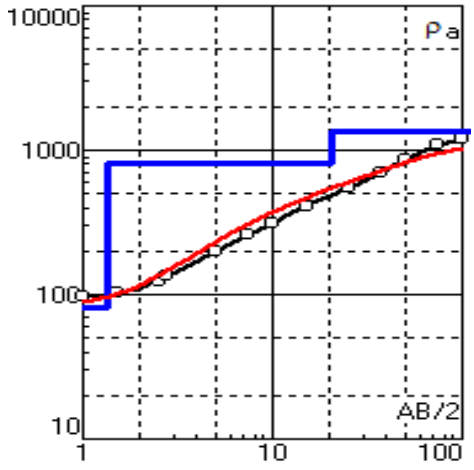



Apparent resistivity (Ωm)

Electrode spacing (m)

CURVE AT VES CT 28 (TYPE A)

| N | ρ | h | d |
|---|---|---|---|
| 1 | 32 | 1.69 | 1.69 |
| 2 | 933 | 7.32 | 9.01 |
| 3 | 1322 | | |
| | | | |

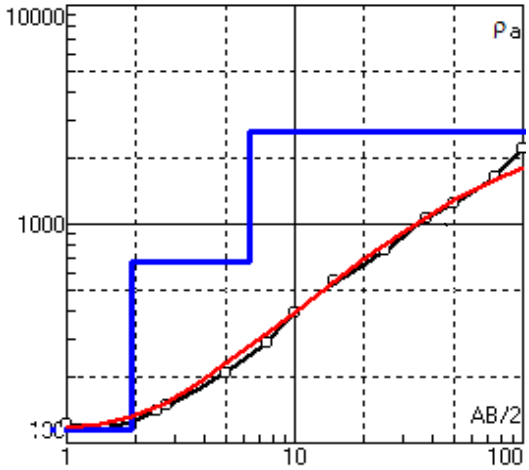



Apparent resistivity (Ωm)

Electrode spacing (m)

CURVE AT CT 29 (TYPE A)

| N | ρ | h | d |
|---|---|---|---|
| 1 | 96 | 1.3 | 1.3 |
| 2 | 588 | 19.5 | 20.8 |
| 3 | 1277 | | |
| | | | |

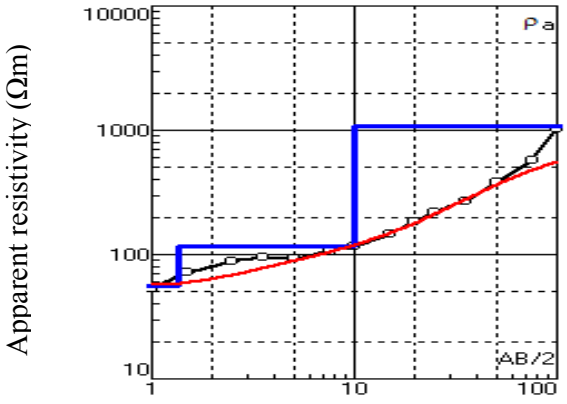



Apparent resistivity (Ωm)

Electrode spacing (m)

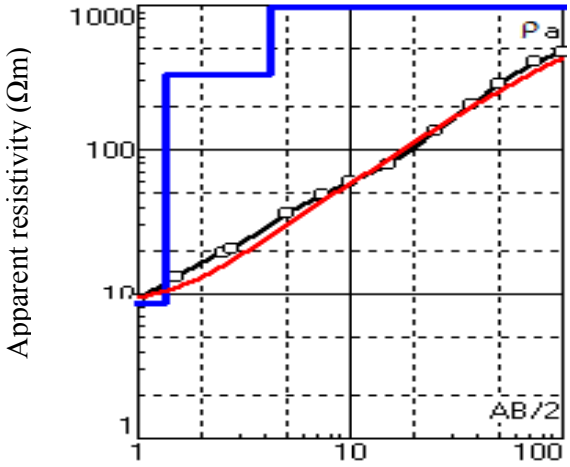
CURVE AT VES CT 30 (TYPE A)

| N | ρ | h | d |
|---|---|---|---|
| 1 | 123 | 1.94 | 1.94 |
| 2 | 987 | 4.34 | 6.28 |
| 3 | 2584 | | |
| | | | |



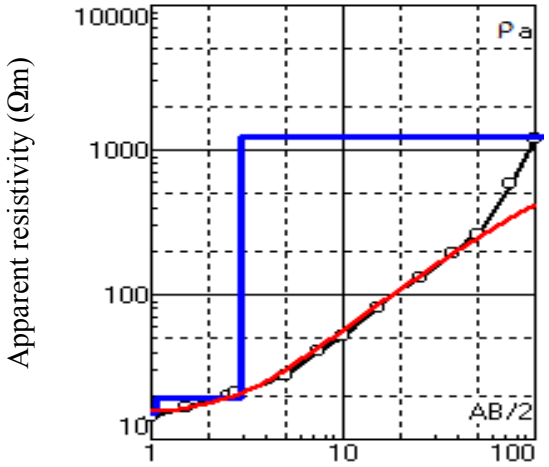

| N | ρ | h | d |
|---|---|---|---|
| 1 | 55 | 1.36 | 1.36 |
| 2 | 116 | 8.64 | 10 |
| 3 | 1072 | | |
| | | | |

CURVE AT VES CT 31 (TYPE A)



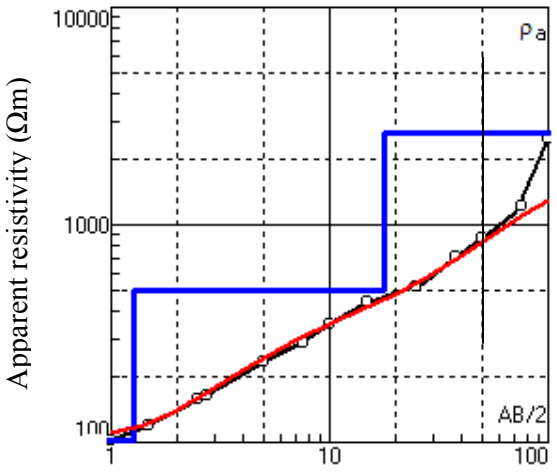

| N | ρ | h | d |
|---|---|---|---|
| 1 | 8 | 1.37 | 1.37 |
| 2 | 336 | 2.67 | 4.04 |
| 3 | 990 | | |
| | | | |

CURVE AT VES CT 32 (TYPE A)



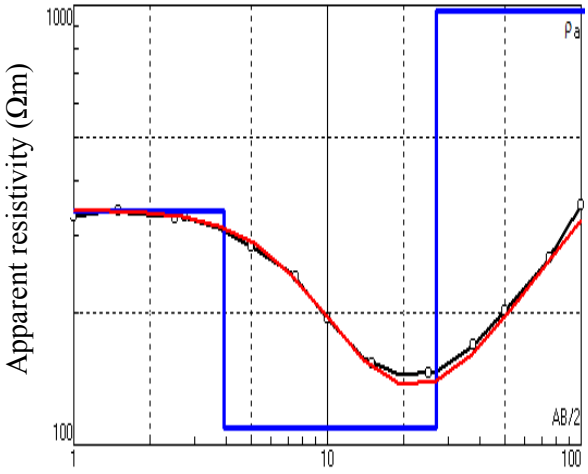

| N | ρ | h | d |
|---|---|---|---|
| 1 | 14 | 1.57 | 1.57 |
| 2 | 275 | 9.04 | 10.61 |
| 3 | 1369 | | |
| | | | |

CURVE AT VES CT 33 (TYPE A)



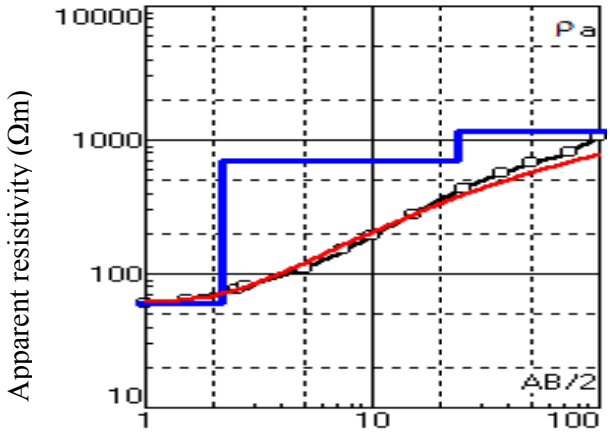

CURVE AT VES CT 34 (TYPE A)

| N | ρ | h | d |
|---|---|---|---|
| 1 | 108 | 1.21 | 1.21 |
| 2 | 546 | 9.42 | 10.63 |
| 3 | 2859 | | |
| | | | |



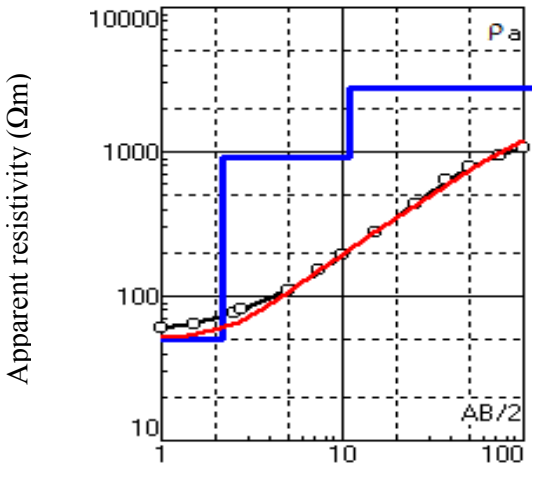

CURVE AT VES CT 35 (TYPE H)

| N | ρ | h | d |
|---|---|---|---|
| 1 | 336 | 3.91 | 3.91 |
| 2 | 159 | 23 | 26.9 |
| 3 | 991 | | |
| | | | |



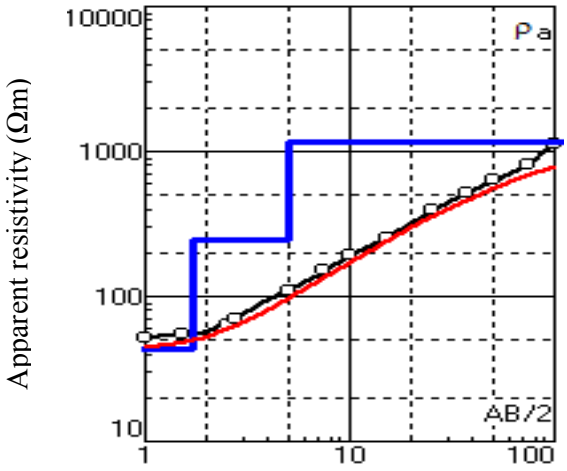

CURVE AT VES CT 36 (TYPE A)

| N | ρ | h | d |
|---|---|---|---|
| 1 | 61 | 2.01 | 2.01 |
| 2 | 613 | 20.5 | 22.51 |
| 3 | 1026 | | |
| | | | |



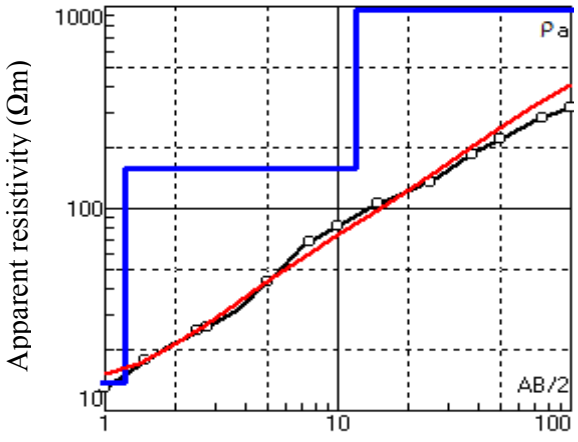

| N | ρ | h | d |
|---|---|---|---|
| 1 | 49 | 2.08 | 2.08 |
| 2 | 966 | 8.83 | 10.91 |
| 3 | 3162 | | |
| | | | |

CURVES AT VES CT 37 (TYPE A)



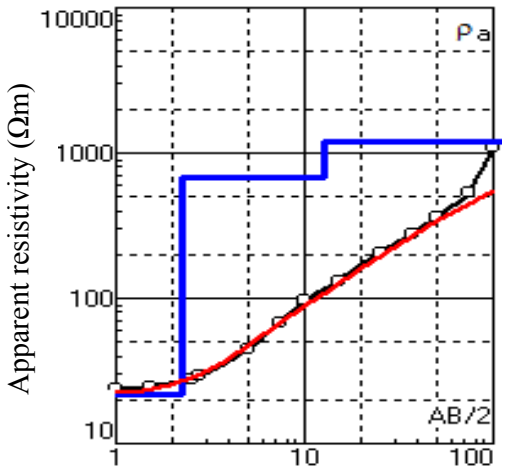

| N | ρ | h | d |
|---|---|---|---|
| 1 | 43 | 1.72 | 1.72 |
| 2 | 248 | 3.43 | 5.15 |
| 3 | 1150 | | |
| | | | |

CURVE AT VES CT 38 (TYPE A)




| N | ρ | h | d |
|---|---|---|---|
| 1 | 13.7 | 1.22 | 1.22 |
| 2 | 158 | 10.7 | 12 |
| 3 | 961 | | |
| | | | |

CURVE AT VES CT 39 (TYPE A)




| N | ρ | h | d |
|---|---|---|---|
| 1 | 24 | 2.24 | 2.24 |
| 2 | 681 | 10.6 | 12.84 |
| 3 | 1150 | | |
| | | | |

CURVE AT VES CT 40 (TYPE A)

Where,

**N** is the layer number,

**ρ** is the layer resistivity in Ωm,

**h** is the layer thickness and

**d** is the depth to the interface in metre.

**Field curve**
**Synthetic curve**
**Model**